Ultrasound in medicine and biology

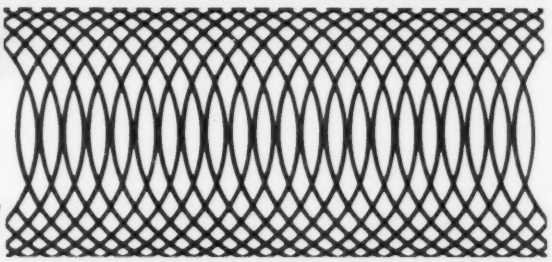

Supplement to *Ultrasound in Medicine and Biology*, Volume 24, Number 7, 1998

Author–Subject Index Volume 23 (1997)

Compiled by

Michael Halliwell

Department of Medical Physics, Bristol General Hospital, Bristol BS1 6SY, United Kingdom

ELSEVIER

ULTRASOUND IN MEDICINE AND BIOLOGY

WORLD FEDERATION FOR ULTRASOUND IN MEDICINE AND BIOLOGY

President: H. LUTZ, *Germany*

Past-President: B. B. GOLDBERG, *USA*

President-Elect: H. WATANABE, *Japan*

Vice-President I: G. CERRI, *Brazil*

Vice-President II: H. Y. CHEN, *Taiwan*

Treasurer: M. C. ZISKIN, *USA*

Secretary: S. HANCKE, *Denmark*

Administrative Councillors:

M. MAKUUCHI, *Japan*

L. BOLONDI, *Italy*

L. PLATT, *USA*

A. BELINSKY, *Argentina*

R. GILL, *Australia*

H. A. GHARBI, *Tunisia*

Co-opted Councillors:

B.-I. CHOI, *Korea*

S. EIK-NES, *Norway*

C. R. B. MERRITT, *USA*

Editor-in-Chief:

P. N. T. WELLS, *UK*

AFFILIATED SOCIETIES

American Institute of Ultrasound in Medicine (AIUM), L. D. Greenbaum, Secretary, 14750 Sweitzer Lane, Suite 100, Laurel, MD 20707, USA

Asian Federation of Societies for Ultrasound in Medicine and Biology (AFSUMB), K. Nakayama, Secretary, Faculty of Science and Technology, Sophia University, 7-1 Kioicho, Chiyoda-ku, Tokyo, Japan

Australasian Society for Ultrasound in Medicine (ASUM), S. Butterworth, Executive Officer, 2/181 High Street, Willoughby, NSW 2068, Australia

European Federation of Societies for Ultrasound in Medicine and Biology (EFSUMB), G. Stanford, General Secretary, Carpenters Court, 4a Lewes Road, Bromley BR1 2RN, United Kingdom

Latin-American Federation of Societies for Ultrasound in Medicine and Biology (FLAUS), G. G. Cerri, Permanent Secretary, Av. Paulista, 491 13° conj. 132, CEP 01311, São Paulo, Brazil

Mediterranean and African Society for Ultrasound (MASU), H. A. Gharbi, Secretary, 12 Ruc Mohamed Salahoddine, 1082 Tunis, Tunisia

For Advertising Orders & Inquiries: North & South America: Jay Allan Feinman, Elsevier Science Inc., 655 Avenue of the Americas, New York, NY 10010. Tel: (212) 633-3689; Fax: (212) 633-3820; E-mail: j.feinman@elsevier.com

International: Advertising Department Elsevier Science, The Boulevard, Langford Lane, Kidlington, Oxford, OX5 1GB, United Kingdom, Tel: (+44) (0) 1865 843565; Fax (44) (0) 1865 843976; E-mail: media@elsevier.co.uk

Japan: Advertising Department Elsevier Science Japan Tel: (81) (3) 5561 5033; Fax: (81) (3) 5561 5047

Published 9 per Annum. *Annual Institutional Subscription Rate* (1998): For customers in Europe, The CIS and Japan: Institutional Rate: NLG 1,427.00. Student/Resident Rate: NLG 101.00. For customers in all other Countries: Institutional Rate: US$820.00. Student/Resident Rate: US$82.00. Prices include postage and are subject to change without notice. Members of the World Federation for Ultrasound in Medicine and Biology may order personal subscriptions at a concessional rate; details of these rates are available upon request.

Any inquiry relating to subscriptions should be sent to: **The Americas:** Elsevier Science, Customer Support Department, P.O. Box 945, New York, NY 10010, USA. [Tel: (+1)212-633-3730/1-888 4ES-INFO. Fax: (+1)212-633-3680. E-mail: usinfo-f@elsevier.com]. **Japan:** Elsevier Science, Customer Support Department, 9-15 Higashi-Azabu 1-chome, Minato-ku, Tokyo 106, Japan [Tel: (+3)5561-5033. Fax: (+3)5561-5047. E-mail: kyf04035@niftyserve.or.jp]. **Asia Pacific (*excluding Japan*):** Elsevier Science (Singapore) Pte Ltd, No. 1 Temasek Avenue, 17-01 Millenia Tower, Singapore 039192. [Tel: (+65)434-3727. Fax: (+65)337-2230. E-mail: asiainfo@elsevier.com.sg]. **Rest of the World:** Elsevier Science, Customer Service Department, P.O. Box 211, 1001 AE Amsterdam, The Netherlands. [Tel: (+31)20-485-3757. Fax: (+31) 20-485-3432. E-mail: nlinfo-f@elsevier.nl].

Please direct inquiries regarding the purchase of reprints to Dan Cronin, Elsevier Science Inc., 655 Avenue of the Americas, New York, NY 10010. Telephone: (212) 633-3813; Fax: (212) 633-3820.

Ultrasound
in medicine
and biology

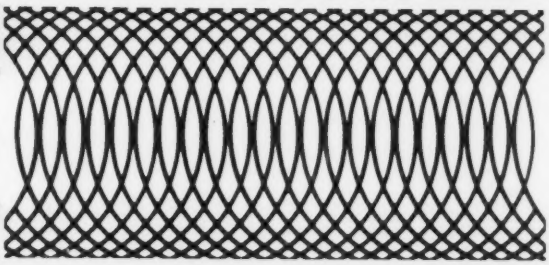

Supplement to *Ultrasound in Medicine and Biology,* Volume 24, Number 7, 1998

Author–Subject Index
Volume 23 (1997)

ELSEVIER

Ultrasound in Med. & Biol., Vol. 24, Suppl., pp. 1–85, 1998
Copyright © 1998 World Federation for Ultrasound in Medicine & Biology
Printed in the USA. All rights reserved
0301-5629/98 $19.00 + .00

PII S0301-5629(98)00067-2

AUTHOR/SUBJECT INDEX

A

A-mode
sonographic determination of cutaneous and subcutaneous fibrosis after accidental exposure to ionising radiation in the course of the Chernobyl nuclear power plant accident (Gottlöber), 9

Abramowicz, J. S.: ultrasound contrast media and their use in obstetrics and gynaecology, 1287

Accuracy
performance of a miniature magnetic position sensor for three-dimensional ultrasound imaging (Leotta), 597

Acoustic bone window
insufficient and absent acoustic temporal bone window: potential and limitations of transcranial contrast-enhanced color-coded sonography and contrast-enhanced power-based sonography (Postert), 857

Acoustic hemostasis
liver hemostasis using high-intensity focused ultrasound (Vaezy), 1413

Acoustic microscope
correlation of ultrasonic attenuation (30 to 50 MHz) and constituents of atherosclerotic plaque (Bridal), 691
high-frequency ultrasonic detection of thrombi with a targeted contrast system (Lanza), 863
influences of ultrasonic machine settings, transducer frequency and placement of region of interest on the measurement of integrated backscatter and cyclic variation (Ota), 1059
parametric (integrated backscatter and attenuation) images constructed using backscattered radiofrequency signals (25–56 MHz) from human aortae *in vitro* (Bridal), 215
ultrasonic tissue characterization of infarcted myocardium by scanning acoustic microscopy (Saijo), 77

Acoustic streaming
a piezocomposite shock-wave generator with electronic focusing capability: application for producing cavitation-induced lesions in rabbit liver (Tavakkoli), 107
acoustic streaming: comparison of low-amplitude linear model with streaming velocities measured by 32-MHz Doppler (Nowicki), 783

Acousto-optics
an optical trigger source for hydrophone-based ultrasound measurement systems: a feasibility study (Petley), 755

Active contour models
interactive automatic fetal head measurements from ultrasound images using multimedia computer technology (Pathak), 665

Adler, D. D., see Carson, P. L.

Adler, R. S., see Chiang, E. H.

Adrenal function
quantitative ultrasound of the heel and serum and urinary cortisol values in assessment of long-term corticotherapy side effects in female bronchial asthma patients (Kos-Kudla), 1325

Age dependence
age dependence of ultrasonically induced lung hemorrhage in mice (Dalecki), 767
ultrasonically induced lung hemorrhage in young swine (Dalecki), 777

Ageing
intra- and extrahepatic arterial resistances in chronic hepatitis and liver cirrhosis (Piscaglia), 675

Agrawal, D., see Anayiotos, A. S.

Agrawal, G., see Anayiotos, A. S.

Ahlgren, A. R., Hansen, F., Sonesson, B. and Länne, T.: stiffness and diameter of the common carotid artery and abdominal aorta in women, 983

Akselrod, S., see Tepper, R.

Alam, S. K. and Ophir, J.: on the use of envelope and RF signal decorrelation as tissue strain estimators, 1427

Albunex
acoustic cavitation nuclei survive the apparent ultrasonic destruction of Albunex microspheres (Brayman), 793
hemolysis of 40% hematocrit, Albunex-supplemented human erythrocytes by pulsed ultrasound: frequency, acoustic pressure and pulse length dependence (Brayman), 1237

Aliasing
color flow mapping (Ferrara), 321

Allard, L., see Cloutier, G.

Allard, L., see Fontaine, I.

Allott, C. P., see Barry, C. D.

Almqvist, M., see Jansson, T.

Amaducci, L., see Marinoni, M.

Ambulatory monitoring
Doppler sensors and harnesses for cardiac and peripheral arterial flow monitoring (Arbeille), 415

Anayiotos, A. S., Elmahdi, A. M., Newman, B. E., Perry, G. J., Costa, F., Agrawal, D., Agrawal, G., DeCarvalho, C. T. and Nanda, N. C.: an improved flow evaluation scheme in orifices of different aspect ratios, 231

Anderson, T., see Spencer, T.

Andreoli, S. P., see Cleveland, R. O.

Aneurysm
ophthalmic artery aneurysms: an investigation by duplex scan (Molnar), 1319

Angle-independent Doppler
feasibility of angle-independent Doppler color imaging for *in vivo* application: preliminary study on carotid arteries (Fei), 59

Anselmo-Franci, J. A., see Haddad, S.

Antich, P., see Mehta, S.

Anticonvulsant therapy
bone status after long-term anticonvulsant therapy in epileptic patients: evaluation using quantitative ultrasound of calcaneus and phalanges (Pluskiewicz), 553

Aorta
correlation of ultrasonic attenuation (30 to 50 MHz) and constituents of atherosclerotic plaque (Bridal), 691
stiffness and diameter of the common carotid artery and abdominal aorta in women (Ahlgren), 983

Aortic pressure
effects of pulsed ultrasound on the frog heart: III. the radiation force mechanism (Dalecki), 275

Apoptosis
ultrasonic biomicroscopy of viable, dead and apoptotic cells (Czarnota), 961

Aquaporins
stress-wave–induced membrane permeation of red blood cells is facilitated by aquaporins (Lee), 1089

Arbeille, P.: Doppler sensors and harnesses for cardiac and peripheral arterial flow monitoring, 415

Arditi, M., Brenier, T. and Schneider, M.: preliminary study in differential contrast echography, 1185

Area index
evaluation of cerebral arterial flow with transcranial Doppler ultrasound: theoretical development and phantom studies (Hatab), 1025

Arefiev, A., see Tavakkoli, J.

Areias, J. C., see Montenegro, N.

Artefact
a study of the quantitative and qualitative impact of catheter shaft angulation in a mechanical intravascular ultrasound system (Kearney), 87
an evaluation of the potential and limitations of three-dimensional reconstructions from intravascular ultrasound images (Thrush), 437
color flow mapping (Ferrara), 321
intravascular elasticity imaging using ultrasound: feasibility studies in phantoms (De Korte), 735

signals from dual gated TCD systems: curious observations and possible explanations (Smith), 15

Arterial diameter
comparison of B-mode, M-mode and echo-tracking methods for measurement of the arterial distension waveform (Stadler), 879
stiffness and diameter of the common carotid artery and abdominal aorta in women (Ahlgren), 983

Arterial disease
an FFT-based flow profiler for high-resolution *in vivo* investigations (Tortoli), 899
neural network analysis of Doppler ultrasound blood-flow signals: a pilot study (Wright), 683

Arterial distensibility
comparison of B-mode, M-mode and echo-tracking methods for measurement of the arterial distension waveform (Stadler), 879

Arterial elasticity
tissue-equivalent vessel phantoms for intravascular ultrasound (Ryan), 261
variation of common carotid artery elasticity with intimal-medial thickness: the ARIC study (Riley), 157

Arterial flow
high-frequency ultrasonic detection of thrombi with a targeted contrast system (Lanza), 863
insufficient and absent acoustic temporal bone window: potential and limitations of transcranial contrast-enhanced color-coded sonography and contrast-enhanced power-based sonography (Postert), 857

Arterial lumen
ultrasound contrast agent in intravascular echography: an *in vitro* study (Cachard), 705

Arterial reconstruction
intraoperative evaluation of small-calibre arterial reconstructions (Sugawara), 473

Arterial resistance
intra- and extrahepatic arterial resistances in chronic hepatitis and liver cirrhosis (Piscaglia), 675

Arteriovenous shunt
Doppler ultrasound in the evaluation of cirrhotic patients: the prevalence of intrahepatic arteriovenous shunting, and implications for diagnosis of hepatocellular carcinoma (Taylor), 1155

Artery
a high-frequency pulsed-wave Doppler ultrasound system for the detection and imaging of blood flow in the microcirculation (Christopher), 997
automated detection of local artery wall thickness based on M-line signal processing (Hoeks), 1017
characterisation of atherosclerotic plaque by spectral analysis of intravascular ultrasound: an *in vitro* methodology (Spencer), 191

comparison of B-mode, M-mode and echo-tracking methods for measurement of the arterial distension waveform (Stadler), 879
contrast ultrasonography for 2-D opacification of heart cavities, peripheral vessels, kidney and muscle (Strauss), 975
correlation of ultrasonic attenuation (30 to 50 MHz) and constituents of atherosclerotic plaque (Bridal), 691
deconvolution process in measurement of arterial velocity profiles *via* an ultrasonic pulsed Doppler velocimeter for evaluation of the wall shear rate (Flaud), 425
differences in the erythrocyte aggregation level between veins and arteries of normolipidemic and hyperlipidemic individuals (Cloutier), 1383
Doppler sensors and harnesses for cardiac and peripheral arterial flow monitoring (Arbeille), 415
feasibility of angle-independent Doppler color imaging for *in vivo* application: preliminary study on carotid arteries (Fei), 59
influence of tissue preservation methods on arterial geometry and echogenicity (Wilhjelm), 1071
neural network analysis of Doppler ultrasound blood-flow signals: a pilot study (Wright), 683
ophthalmic artery aneurysms: an investigation by duplex scan (Molnar), 1319
parametric (integrated backscatter and attenuation) images constructed using backscattered radiofrequency signals (25–56 MHz) from human aortae *in vitro* (Bridal), 215
peak velocity estimation in arterial stenosis models using colour vector Doppler (Hoskins), 889
reproducibility of shear rate and shear stress assessment by means of ultrasound in the common carotid artery of young human males and females (Samijo), 583
stiffness and diameter of the common carotid artery and abdominal aorta in women (Ahlgren), 983
the reproducibility of color Doppler duplex sonography in the measurement of renal arterial blood velocity (Imuta), 813
tissue-equivalent vessel phantoms for intravascular ultrasound (Ryan), 261
ultrasound contrast agent in intravascular echography: an *in vitro* study (Cachard), 705
unusual pseudoaneurysms after catheterization: successful treatment by ultrasound-guided compression (Do), 377
variation of common carotid artery elasticity with intimal-medial thickness: the ARIC study (Riley), 157

Articular cartilage
ultrasonic characterization of *in vitro* osteoarthritic articular cartilage with validation by confocal microscopy (Chiang), 205

Arundel, P. A., see Barry, C. D.

A-Scan
ultrasound in ophthalmology (Fledelius), 365

Astor, M., see Lizzi, F. L.

Atherosclerosis
characterisation of atherosclerotic plaque by spectral analysis of intravascular ultrasound: an *in vitro* methodology (Spencer), 191

correlation of ultrasonic attenuation (30 to 50 MHz) and constituents of atherosclerotic plaque (Bridal), 691
intravascular elasticity imaging using ultrasound: feasibility studies in phantoms (de Korte), 735
parametric (integrated backscatter and attenuation) images constructed using backscattered radiofrequency signals (25–56 MHz) from human aortae *in vitro* (Bridal), 215
variation of common carotid artery elasticity with intimal-medial thickness: the ARIC study (Riley), 157

Atrial fibrillation
direct effects of DC cardioversion on blood echogenicity: an *in vitro* study (Fatkin), 135

Atrial stunning
direct effects of DC cardioversion on blood echogenicity: an *in vitro* study (Fatkin), 135

Attenuation
automatic attenuation compensation for ultrasonic imaging (Hughes), 651
correlation of ultrasonic attenuation (30 to 50 MHz) and constituents of atherosclerotic plaque (Bridal), 691
measurement of velocity and attenuation of shear waves in bovine compact bone using ultrasonic spectroscopy (Wu), 129
on the use of envelope and RF signal decorrelation as tissue strain estimators (Alam), 1427
parametric (integrated backscatter and attenuation) images constructed using backscattered radiofrequency signals (25–56 MHz) from human aortae *in vitro* (Bridal), 215
quantitative acoustic characterization of a new surfactant-based ultrasound contrast agent (Forsberg), 1201
quantitative ultrasound of the heel and serum and urinary cortisol values in assessment of long-term corticotherapy side effects in female bronchial asthma patients (Kos-Kudla), 1325
the assessment of development of bone mass in children by quantitative ultrasound through the proximal phalanxes of the hand (Halaba), 1331
the nonstationary strain filter in elastography: Part I. frequency-dependent attenuation (Varghese), 1343
the nonstationary strain filter in elastography: Part II. lateral and elevational decorrelation (Kallel), 1357
ultrasonic tissue characterization of infarcted myocardium by scanning acoustic microscopy (Saijo), 77
ultrasound attenuation and backscatter in the liver during prednisone administration (Lu), 1
ultrasound properties of liver tissue during heating (Gertner), 1395

Attenuation compensation
automatic attenuation compensation for ultrasonic imaging (Hughes), 651

Automated quality assurance
phantoms and automated system for testing the resolution of ultrasound scanners (Rownd), 245

Automatic TGC
automatic attenuation compensation for ultrasonic imaging (Hughes), 651

Autoregressive model
a study of the spectral broadening of simulated Doppler signals using FFT and AR modelling (Keeton), 1033
recursive autoregressive spectral maps for ocular pathology detection (Fort), 391

A-wave transit time
assessment of mitral A-wave transit time to cardiac outflow tract and isovolumic relaxation time of left ventricle in the appropriate and small-for-gestational-age human fetus (Tsyvian), 187

Azadniv, M., see Everbach, E. C.

B

Backscatter
automatic attenuation compensation for ultrasonic imaging (Hughes), 651
carotid plaque typing by multiparameter ultrasonic tissue characterization (Noritomi), 643
correlation of ultrasonic attenuation (30 to 50 MHz) and constituents of atherosclerotic plaque (Bridal), 691
correlation of ultrasound parameter imaging with microcirculatory patterns in uveal melanomas (Silverman), 573
detection and clinical significance of red cell aggregation in the human subcutaneous vein using a high-frequency transducer (10 MHz): a preliminary report (Kitamura), 933
differences in the erythrocyte aggregation level between veins and arteries of normolipidemic and hyperlipidemic individuals (Cloutier), 1383
high-frequency ultrasonic detection of thrombi with a targeted contrast system (Lanza), 863
influence of data processing on cyclic variation of integrated backscatter and wall thickness in stunned porcine myocardium (van der Steen), 405
influence of tissue preservation methods on arterial geometry and echogenicity (Wilhjelm), 1071
influences of ultrasonic machine settings, transducer frequency and placement of region of interest on the measurement of integrated backscatter and cyclic variation (Ota), 1059
measurement of shear-wave velocity by ultrasound critical-angle reflectometry (UCR) (Mehta), 1123
nonGaussian statistical property of the ultrasonic Doppler signal downstream of a severe stenosis (Fontaine), 41
parametric (integrated backscatter and attenuation) images constructed using backscattered radiofrequency signals (25–56 MHz) from human aortae *in vitro* (Bridal), 215
preliminary study in differential contrast echography (Arditi), 1185
quantitative acoustic characterization of a new surfactant-based ultrasound contrast agent (Forsberg), 1201
recursive autoregressive spectral maps for ocular pathology detection (Fort), 391
statistical framework for ultrasonic spectral parameter imaging (Lizzi), 1371
ultrasonic biomicroscopy of viable, dead and apoptotic cells (Czarnota), 961
ultrasonic characterization of *in vitro* osteoarthritic articular cartilage with validation by confocal microscopy (Chiang), 205
ultrasonic characterization of tissues *via* backscatter frequency dependence (Stetson), 989

ultrasound attenuation and backscatter in the liver during prednisone administration (Lu), 1
ultrasound properties of liver tissue during heating (Gertner), 1395

Backscatter microscope
a high-frequency pulsed-wave Doppler ultrasound system for the detection and imaging of blood flow in the microcirculation (Christopher), 997

Bahner, M. L., see Delorme, S.

Baker, A. C.: a numerical study of the effect of drive level on the intensity loss from an ultrasonic beam, 1083

Bao, S., Thrall, B. D. and Miller, D. L.: transfection of a reporter plasmid into cultured cells by sonoporation *in vitro*, 953

Barkhuysen, R., see Samijo, S. K.

Barned, S. L., see Brayman, A. A.

Barnes, R. W., see Riley, W. A.

Barnett, S. B., Rott, H-D., ter Haar, G. R., Ziskin, M. C. and Maeda, K.: the sensitivity of biological tissue to ultrasound, 805

Barros, H., see Montenegro, N.

Barry, C. D., Allott, C. P., John, N. W., Mellor, P. M., Arundel, P. A., Thomson, D. S. and Waterton, J. C.: three-dimensional freehand ultrasound: image reconstruction and volume analysis, 1209

Basal cerebral arteries
insufficient and absent acoustic temporal bone window: potential and limitations of transcranial contrast-enhanced color-coded sonography and contrast-enhanced power-based sonography (Postert), 857

Bascom, P. A. J., Johnston, K. W., Cobbold, R. S. C. and Ohja, M.: relation of the flow field distal to a moderate stenosis to the Doppler power, 25

Beach, K. W., Comess, K. A., Primozich, J. F., Yuan, C., Powell, K., Phillips, D. J., Dunmire, B., Plett, M., Brown, K., Paun, M. and Strandness, D. E. Jr.: ultrasonic color flow mapping: the visualization of four-dimensional cardiac and vascular flow phenomena using two dimensions and "real time," 347

Beach, K. W.: color flow mapping and hemodynamics, 319

Beach, K., see Vaezy, S.

Beam profile
effects of pulsed ultrasound on the frog heart: III. the radiation force mechanism (Dalecki), 275
thresholds for fetal hemorrhages produced by a piezoelectric lithotripter (Dalecki), 287

Beam shape
a thermal beam-shape phantom for ultrasound physiotherapy transducers (Martin), 1267

Beaulieu, R., see Cloutier, G.

Beller, K-D., see Strauss, A. L.

Benchimol, S., see Czarnota, G. J.

Benign prostatic hypertrophy
preliminary results of power Doppler imaging in benign prostatic hyperplasia (Kojima), 1305

Bensalah, A., see Flaud, P.

Berger, G., see Bridal, S. L.

Berti, P., see Tortoli, T.

Bettlach, J., see Hall, A. F.

Beyer, B.: ultrasonic measurements and technologies: sensor physics and technology series 4, 1442

Beyth, Y., see Tepper, R.

Bilgen, M., see Kallel, F.

Bioeffect
a numerical study of the effect of drive level on the intensity loss from an ultrasonic beam (Baker), 1083
a piezocomposite shock-wave generator with electronic focusing capability: application for producing cavitation-induced lesions in rabbit liver (Tavakkoli), 107
acoustic cavitation nuclei survive the apparent ultrasonic destruction of Albunex microspheres (Brayman), 793
age dependence of ultrasonically induced lung hemorrhage in mice (Dalecki), 767
comparative sensitivity of human erythrocytes and lymphocytes to sonolysis by 1-MHz ultrasound (Miller), 635
correlation of ultrasound-induced hemolysis with cavitation detector output *in vitro* (Everbach), 619
effect of ultrasound on the contraction of isolated myocardial cells of adult rats (Salz), 143
effects of pulsed ultrasound on the frog heart: III. the radiation force mechanism (Dalecki), 275
hemolysis *in vivo* from exposure to pulsed ultrasound (Dalecki), 315
hemolysis of 40% hematocrit, Albunex-supplemented human erythrocytes by pulsed ultrasound: frequency, acoustic pressure and pulse-length–dependence (Brayman), 1237
liver hemostasis using high-intensity focused ultrasound (Vaezy), 1413
minimal static excess pressure minimises the effect of extracorporeal shock waves on cells and reduces it on gallstones (Delius), 611
quantitation of shock-wave cavitation damage *in vitro* (Lifshitz), 461
remnants of Albunex nucleate acoustic cavitation (Dalecki), 1405
stress-wave–induced membrane permeation of red blood cells is facilitated by aquaporins (Lee), 1089
temperature rise recorded during lesion formation by high-intensity focused ultrasound (Clarke), 299
the effect of polypropylene vials on lithotripter shock waves (Cleveland), 939
the influence of contrast agents on hemorrhage produced by lithotripter fields (Dalecki), 1435
the sensitivity of biological tissue to ultrasound (Barnett), 805
thresholds for fetal hemorrhages produced by a piezoelectric lithotripter (Dalecki), 287
thresholds for premature contractions in murine hearts exposed to pulsed ultrasound (MacRobbie), 761

transfection of a reporter plasmid into cultured cells by sonoporation *in vitro* (Bao), 953
ultrasonically induced hemolysis at high cell and gas body concentrations in a thin-disc exposure chamber (Miller), 625
ultrasonically induced lung hemorrhage in young swine (Dalecki), 777
ultrasound contrast media and their use in obstetrics and gynecology (Abramowicz), 1287
ultrasound properties of liver tissue during heating (Gertner), 1395
ultrasound stimulation of rat testes damaged by Busulfan (Haddad), 1421

Biometry
ultrasonographic biometry in salivary glands (Dost), 1299

Biomicroscope
a high-frequency pulsed-wave Doppler ultrasound system for the detection and imaging of blood flow in the microcirculation (Christopher), 997
correlation of ultrasonic attenuation (30 to 50 MHz) and constituents of atherosclerotic plaque (Bridal), 691
parametric (integrated backscatter and attenuation) images constructed using backscattered radiofrequency signals (25–56 MHz) from human aortae *in vitro* (Bridal), 215
ultrasonic biomicroscopy of viable, dead and apoptotic cells (Czarnota), 961
ultrasonic characterization of *in vitro* osteoarthritic articular cartilage with validation by confocal microscopy (Chiang), 205
ultrasonic tissue characterization of infarcted myocardium by scanning acoustic microscopy (Saijo), 77
ultrasound in ophthalmology (Fledelius), 365

Biopsy
lack of correlation between ultrasonography and histologic staging of the endometrium in *in vitro* fertilization (IVF) patients (Sterzik), 165
thoraxsonography—part II: peripheral pulmonary consolidation (Mathis), 1141
unusual pseudoaneurysms after catheterization: successful treatment by ultrasound-guided compression (Do), 377

Biorheology
differences in the erythrocyte aggregation level between veins and arteries of normolipidemic and hyperlipidemic individuals (Cloutier), 1383

Birer, A., see Tavakkoli, J.

Birkeland, S., see Zhou, Y-Q.

Bleeding control
liver hemostasis using high-intensity focused ultrasound (Vaezy), 1413

Blood
characterisation of red and white thrombus by intravascular ultrasound using radiofrequency and videodensitometric data-based texture analysis (Ramo), 1195
differences in the erythrocyte aggregation level between veins and arteries of normolipidemic and hyperlipidemic individuals (Cloutier), 1383

Blood cells
the sensitivity of biological tissue to ultrasound (Barnett), 805

Blood flow
a radiofrequency domain complex cross-correlation model to estimate blood flow velocity and tissue motion by means of ultrasound (Brands), 911
color flow mapping (Ferrara), 321
colour velocity flow measurement: *in vitro* validation and application to human carotid (Deane), 447
contrast ultrasonography for 2-D opacification of heart cavities, peripheral vessels, kidney and muscle (Strauss), 975
critical comparison of indices and threshold values for assessing placenta performance using Doppler ultrasound (Joern), 1179
decay constant of Doppler flow waveform as a possible indicator of ovarian malignancy (Tepper), 1171
deconvolution process in measurement of arterial velocity profiles *via* an ultrasonic pulsed Doppler velocimeter for evaluation of the wall shear rate (Flaud), 425
differences in the erythrocyte aggregation level between veins and arteries of normolipidemic and hyperlipidemic individuals (Cloutier), 1383
Doppler sensors and harnesses for cardiac and peripheral arterial flow monitoring (Arbeille), 415
ductus venosus revisited: a Doppler blood flow evaluation in the first trimester of pregnancy (Montenegro), 171
echo machine-imposed limit on transmitral spectral Doppler velocity-profile analysis (Hall), 1225
evaluation of cerebral arterial flow with transcranial Doppler ultrasound: theoretical development and phantom studies (Hatab), 1025
gray-scale second harmonic imaging of the liver: a preliminary animal study (Kono), 719
neural network analysis of Doppler ultrasound blood flow signals: a pilot study (Wright), 683
new signs of breast cancer: high resistance flow and variations in resistive indices evaluation by color Doppler sonography (Hollerweger), 851
nonGaussian statistical property of the ultrasonic Doppler signal downstream of a severe stenosis (Fontaine), 41
ophthalmic artery aneurysms: an investigation by duplex scan (Molnar), 1319
peak velocity estimation in arterial stenosis models using colour vector Doppler (Hoskins), 889
rapid measurement of the spatial resolution of colour flow scanners (Li), 591
reproducibility of shear rate and shear stress assessment by means of ultrasound in the common carotid artery of young human males and females (Samijo), 583
the 3-D and 2-D color flow display of breast masses (Carson), 837
the reproducibility of color Doppler duplex sonography in the measurement of renal arterial blood velocity (Imuta), 813
ultrasonic color flow mapping: the visualization of four-dimensional cardiac and vascular flow phenomena using two dimensions and "real time" (Beach), 347
ultrasound Doppler vector tomography measurements of directional blood flow (Jansson), 47

Blood flow profiles
an FFT-based flow profiler for high-resolution *in vivo* investigations (Tortoli), 899

Blood velocity
a high-frequency pulsed-wave Doppler ultrasound system for the detection and imaging of blood flow in the microcirculation (Christopher), 997
an FFT-based flow profiler for high-resolution *in vivo* investigations (Tortoli), 899
clinical application of hepatic venous hemodynamics by Doppler ultrasonography in chronic liver disease (Hamato), 829
color flow mapping (Ferrara), 321
estimation of axial blood velocity using the Doppler equation corrected for broadening (Chabria), 967
peak velocity estimation in arterial stenosis models using colour vector Doppler (Hoskins), 889
phase shift of the hepatic vein flow velocity waveform in chronic liver disease: experimental and clinical studies (Hamato), 821
the reproducibility of color Doppler duplex sonography in the measurement of renal arterial blood velocity (Imuta), 813
ultrasonic color flow mapping: the visualization of four-dimensional cardiac and vascular flow phenomena using two dimensions and "real time" (Beach), 347

Blood viscosity
reproducibility of shear rate and shear stress assessment by means of ultrasound in the common carotid artery of young human males and females (Samijo), 583

Blood volume
the 3-D and 2-D color flow display of breast masses (Carson), 837

Blott, B. H., see Petley, G. W.

Boes, J. L., see Chiang, E. H.

Boldt, H. C., see Silverman, R. H.

Bolondi, L., see Piscaglia, F.

Bom, N., see van der Steen, A. F. W.

Bond, A. D., see Preston, R. C.

Bone
a novel method to measure acoustic speed of bone tissue (Chen), 1337
bone status after long-term anticonvulsant therapy in epileptic patients: evaluation using quantitative ultrasound of calcaneus and phalanges (Pluskiewicz), 553
insufficient and absent acoustic temporal bone window: potential and limitations of transcranial contrast-enhanced color-coded sonography and contrast-enhanced power-based sonography (Postert), 857
measurement of shear-wave velocity by ultrasound critical-angle reflectometry (UCR) (Mehta), 1123
measurement of velocity and attenuation of shear waves in bovine compact bone using ultrasonic spectroscopy (Wu), 129
quantitative ultrasound of the heel and serum and urinary cortisol values in assessment of long-term corticotherapy side effects in female bronchial asthma patients (Kos-Kudla), 1325
the assessment of development of bone mass in children by quantitative ultrasound through the proximal phalanxes of the hand (Halaba), 1331

the stimulation of bone formation *in vitro* by therapeutic ultrasound (Reher), 1251

Bone healing
the stimulation of bone formation *in vitro* by therapeutic ultrasound (Reher), 1251

Bonnett, D. E., see Thrush, A. J.

Bouakaz, A., see Cachard, C.

Boutouyrie, P., see Hoeks, A. P. G.

Bovine
a novel method to measure acoustic speed of bone tissue (Chen), 1337
measurement of velocity and attenuation of shear waves in bovine compact bone using ultrasonic spectroscopy (Wu), 129

Brachial artery
unusual pseudoaneurysms after catheterization: successful treatment by ultrasound-guided compression (Do), 377

Brands, P. J., Hoeks, A. P. G., Ledoux, L. A. F. and Reneman, R. S.: a radio frequency domain complex cross-correlation model to estimate blood flow velocity and tissue motion by means of ultrasound, 911

Brands, P. J., see Hoeks, A. P. G.

Brands, P. J., see Samijo, S. K.

Brayman, A. A. and Miller, M. W.: acoustic cavitation nuclei survive the apparent ultrasonic destruction of Albunex microspheres, 793

Brayman, A. A., see Miller, W. M.

Brayman, A. A., Strickler, P. L., Luan, H., Barned, S. L., Raeman, C. H., Cox, C. and Miller, M. W.: hemolysis of 40% hematocrit, Albunex-supplemented human erythrocytes by pulsed ultrasound: frequency, acoustic pressure and pulse length dependence, 1237

Breast
new signs of breast cancer: high resistance flow and variations in resistive indices evaluation by color Doppler sonography (Hollerweger), 851
the 3-D and 2-D color flow display of breast masses (Carson), 837
ultrasonic measurement of breast tissue motion and the implications for velocity estimation (El-Fallah), 1047
ultrasound Doppler vector tomography measurements of directional blood flow (Jansson), 47

Breast cancer
new signs of breast cancer: high resistance flow and variations in resistive indices evaluation by color Doppler sonography (Hollerweger), 851
the 3-D and 2-D color flow display of breast masses (Carson), 837

Brenier, T., see Arditi, M.

Bridal, S. L., Fornès, P., Bruneval, P. and Berger, G.: correlation of ultrasonic attenuation (30 to 50 MHz) and constituents of atherosclerotic plaque, 691

Bridal, S. L., Fornès, P., Bruneval, P. and Berger, G.: parametric (integrated backscatter and attenuation) images constructed using backscattered radiofrequency signals (25–56 MHz) from human aortae *in vitro*, 215

Brode, S. E., see Ren, J-F.

Bronchial asthma
quantitative ultrasound of the heel and serum and urinary cortisol values in assessment of long-term corticotherapy side effects in female bronchial asthma patients (Kos-Kudla), 1325

Brown, K., see Beach, K. W.

Bruneval, P., see Bridal, S. L.

Bubbles
direct effects of DC cardioversion on blood echogenicity: an *in vitro* study (Fatkin), 135

Burke, G. L., see Riley, W. A.

Burns, P. N., see Christopher, D. A.

Büttner, T., see Postert, T.

C

Cachard, C., Finet, G., Bouakaz, A., Tabib, A., Francon, D. and Gimenez, G.: ultrasound contrast agent in intravascular echography: an *in vitro* study, 705

Cacheris, W. P., see Lanza, G. M.

Calcaneus
bone status after long-term anticonvulsant therapy in epileptic patients: evaluation using quantitative ultrasound of calcaneus and phalanges (Pluskiewicz), 553

Caldas, J. G. M. P., see Molnar, L. J.

Calibration
an optical trigger source for hydrophone-based ultrasound measurement systems: a feasibility study (Petley), 755

Cancer
a piezocomposite shock-wave generator with electronic focusing capability: application for producing cavitation-induced lesions in rabbit liver (Tavakkoli), 107
decay constant of Doppler flow waveform as a possible indicator of ovarian malignancy (Tepper), 1171
gray-scale second harmonic imaging of the liver: a preliminary animal study (Kono), 719
influence of ablated tissue on the formation of high-intensity focused ultrasound lesions (Chen), 921
new signs of breast cancer: high resistance flow and variations in resistive indices evaluation by color Doppler sonography (Hollerweger), 851
prognostic significance of color Doppler findings in head and neck tumors (Delorme), 1311
the 3-D and 2-D color flow display of breast masses (Carson), 837
ultrasound contrast media and their use in obstetrics and gynecology (Abramowicz), 1287
ultrasound properties of liver tissue during heating (Gertner), 1395

Caps, M., see Vaezy, S.

Cardiac-induced movement
ultrasonic measurement of breast tissue motion and the implications for velocity estimation (El-Fallah), 1047

Cardiac muscle
thresholds for premature contractions in murine hearts exposed to pulsed ultrasound (MacRobbie), 761

Cardiac outflow tract
assessment of mitral A-wave transit time to cardiac outflow tract and isovolumic relaxation time of left ventricle in the appropriate and small-for–gestational–age human fetus (Tsyvian), 187

Cardiac output
Doppler sensors and harnesses for cardiac and peripheral arterial flow monitoring (Arbeille), 415
effects of velocity distribution, diameter measurement and velocity tracing on the accuracy of cardiac output measurement by pulsed Doppler echocardiography in the aortic annulus of pigs (Zhou), 177

Cardiac stroke volume
Doppler sensors and harnesses for cardiac and peripheral arterial flow monitoring (Arbeille), 415

Cardiography
Doppler myocardial imaging vs. B-mode grey-scale imaging: a comparative *in vitro* and *in vivo* study into their relative efficacy in endocardial boundary detection (Lange), 69
ultrasonic color flow mapping: the visualization of four-dimensional cardiac and vascular flow phenomena using two dimensions and "real time" (Beach), 347

Cardiovascular monitoring
Doppler sensors and harnesses for cardiac and peripheral arterial flow monitoring (Arbeille), 415

Cardioversion
direct effects of DC cardioversion on blood echogenicity: an *in vitro* study (Fatkin), 135

Carotid artery
a study of the spectral broadening of simulated Doppler signals using FFT and AR modelling (Keeton), 1033
automated detection of local artery wall thickness based on M-line signal processing (Hoeks), 1017
carotid plaque typing by multiparameter ultrasonic tissue characterization (Noritomi), 643
colour velocity flow measurement: *in vitro* validation and application to human carotid (Deane), 447
comparison of B-mode, M-mode and echo-tracking methods for measurement of the arterial distension waveform (Stadler), 879
Doppler sensors and harnesses for cardiac and peripheral arterial flow monitoring (Arbeille), 415
feasibility of angle-independent Doppler color imaging for *in vivo* application: preliminary study on carotid arteries (Fei), 59

neural network analysis of Doppler ultrasound blood flow signals: a pilot study (Wright), 683
reproducibility of shear rate and shear stress assessment by means of ultrasound in the common carotid artery of young human males and females (Samijo), 583
stiffness and diameter of the common carotid artery and abdominal aorta in women (Ahlgren), 983
three-dimensional freehand ultrasound: image reconstruction and volume analysis (Barry), 1209
ultrasonic color flow mapping: the visualization of four-dimensional cardiac and vascular flow phenomena using two dimensions and "real time" (Beach), 347
variation of common carotid artery elasticity with intimal-medial thickness: the ARIC study (Riley), 157

Carotid bifurcation
feasibility of angle-independent Doppler color imaging for *in vivo* application: preliminary study on carotid arteries (Fei), 59

Carotid stenosis
a study of the spectral broadening of simulated Doppler signals using FFT and AR modelling (Keeton), 1033

Carson, P. L., Moskalik, A. P., Govil, A., Roubidoux, M. A., Fowlkes, J. B., Normolle, D., Adler, D. D., Rubin, J. M. and Helvie, M.: the 3-D and 2-D color flow display of breast masses, 837

Carstensen, E. L., see Dalecki, D.

Carter, S., see Vaezy, S.

Cartilage
ultrasonic characterization of *in vitro* osteoarthritic articular cartilage with validation by confocal microscopy (Chiang), 205

Carvalho, T. L. L., see Haddad, S.

Casali, A., see Piscaglia, F.

Case, C. Q., see Taylor, C. R.

Caso, P., see Lange, A.

Cataract surgery
ultrasound in ophthalmology (Fledelius), 365

Catheterization
unusual pseudoaneurysms after catheterization: successful treatment by ultrasound-guided compression (Do), 377

Cathignol, D., see Tavakkoli, J.

Cavitation
a piezocomposite shock-wave generator with electronic focusing capability: application for producing cavitation-induced lesions in rabbit liver (Tavakkoli), 107
acoustic cavitation nuclei survive the apparent ultrasonic destruction of Albunex microspheres (Brayman), 793
correlation of ultrasound-induced hemolysis with cavitation detector output *in vitro* (Everbach), 619

hemolysis *in vivo* from exposure to pulsed ultrasound (Dalecki), 315
hemolysis of 40% hematocrit, Albunex-supplemented human erythrocytes by pulsed ultrasound: frequency, acoustic pressure and pulse-length–dependence (Brayman), 1237
in vitro study of the mechanical effects of shock-wave lithotripsy (Howard), 1107
mechanism of ultrasound-enhanced porphyrin cytotoxicity. Part I: a search for free radical effects (Worthington), 1095
minimal static excess pressure minimises the effect of extracorporeal shock waves on cells and reduces it on gallstones (Delius), 611
quantitation of shock-wave cavitation damage *in vitro* (Lifshitz), 461
remnants of Albunex nucleate acoustic cavitation (Dalecki), 1405
temperature rise recorded during lesion formation by high-intensity focused ultrasound (Clarke), 299
the sensitivity of biological tissue to ultrasound (Barnett), 805
thresholds for fetal hemorrhages produced by a piezoelectric lithotripter (Dalecki), 287
thresholds for premature contractions in murine hearts exposed to pulsed ultrasound (MacRobbie), 761
transfection of a reporter plasmid into cultured cells by sonoporation *in vitro* (Bao), 953
ultrasonically induced hemolysis at high cell and gas body concentrations in a thin-disc exposure chamber (Miller), 625

Cavitation detection
correlation of ultrasound-induced hemolysis with cavitation detector output *in vitro* (Everbach), 619

Cavitation nuclei
acoustic cavitation nuclei survive the apparent ultrasonic destruction of Albunex microspheres (Brayman), 793

Cell damage
acoustic cavitation nuclei survive the apparent ultrasonic destruction of Albunex microspheres (Brayman), 793
comparative sensitivity of human erythrocytes and lymphocytes to sonolysis by 1-MHz ultrasound (Miller), 635
correlation of ultrasound-induced hemolysis with cavitation detector output *in vitro* (Everbach), 619
hemolysis *in vivo* from exposure to pulsed ultrasound (Dalecki), 315
hemolysis of 40% hematocrit, Albunex-supplemented human erythrocytes by pulsed ultrasound: frequency, acoustic pressure and pulse-length–dependence (Brayman), 1237
mechanism of ultrasound enhanced porphyrin cytotoxicity. Part I: a search for free radical effects (Worthington), 1095
minimal static excess pressure minimises the effect of extracorporeal shock waves on cells and reduces it on gallstones (Delius), 611
quantitation of shock-wave cavitation damage *in vitro* (Lifshitz), 461
the effect of polypropylene vials on lithotripter shock waves (Cleveland), 939
ultrasonically induced hemolysis at high cell and gas body concentrations in a thin-disc exposure chamber (Miller), 625

Cell membrane
minimal static excess pressure minimises the effect of extracorporeal shock waves on cells and reduces it on gallstones (Delius), 611

stress-wave induced membrane permeation of red blood cells is facilitated by aquaporins (Lee), 1089

Cerebral arteries
analysis of the frequency modulation present in Doppler ultrasound signals may allow differentiation between particulate and gaseous cerebral emboli (Smith), 727
colour velocity flow measurement: *in vitro* validation and application to human carotid (Deane), 447
evaluation of cerebral arterial flow with transcranial Doppler ultrasound: theoretical development and phantom studies (Hatab), 1025
insufficient and absent acoustic temporal bone window: potential and limitations of transcranial contrast-enhanced color-coded sonography and contrast-enhanced power-based sonography (Postert), 857

Cerebral artery flow
evaluation of cerebral arterial flow with transcranial Doppler ultrasound: theoretical development and phantom studies (Hatab), 1025

Cerebral embolism
analysis of the frequency modulation present in Doppler ultrasound signals may allow differentiation between particulate and gaseous cerebral emboli (Smith), 727

Cerri, G. G., see Molnar, L. J.

Céspedes, E. I., see De Korte, C. L.

Chabria, Y. and Newhouse, V. L.: estimation of axial blood velocity using the Doppler equation corrected for broadening, 967

Chalana, V., see Pathak, S. D.

Chandler.W., see Vaezy, S.

Chang, C-H., see Chang, F-M.

Chang, F-M., Hsu, K-F., Ko, H-C., Yao, B-L., Chang, C-H., Yu, C-H. and Chen, H-Y.: three-dimensional ultrasound assessment of fetal liver volume in normal pregnancy: a comparison of reproducibility with two-dimensional ultrasound and a search for a volume constant, 381

Chapelon, J-Y., see Tavakkoli, J.

Chatterjee, T., see Do, D-D.

Chaudhry, F. A., see Ren, J-F.

Chemical kinetics
an FFT-based flow profiler for high-resolution *in vivo* investigations (Tortoli), 899

Chen, H-Y., see Chang, F-M.

Chen, L., ter Haar, G. and Hill, C. R.: influence of ablated tissue on the formation of high-intensity focused ultrasound lesions, 921

Chen, T., Tzeng, J-S. and Lin, C-J.: a novel method to measure acoustic speed of bone tissue, 1337

Chen, X., see Noritomi, T.

Chen, Y-W., Jeng, J-S., Liu, H-M., Yip, P-K., Hwang, B-S., Lin, W-H., Chang, Y-C. and Tu, Y-K.: Ultrasound in Medicine and Biology Clinical Prize 1996, 1283

Chernobyl
sonographic determination of cutaneous and subcutaneous fibrosis after accidental exposure to ionising radiation in the course of the Chernobyl nuclear power plant accident (Gottlöber), 9

Chest
thoraxsonography—part I: chest wall and pleura (Mathis), 1131
thoraxsonography—part II: peripheral pulmonary consolidation (Mathis), 1141

Chiang, E. H., Laing, T. J., Meyer, C. R., Boes, J. L., Rubin, J. M. and Adler, R. S.: ultrasonic characterization of *in vitro* osteoarthritic articular cartilage with validation by confocal microscopy, 205

Chiba, T., see Hamato, N.

Chiba, T., see Kono, Y.

Child, S. Z., see Dalecki, D.

Child, S. Z., see MacRobbie, A. G.

Cholesterol
detection and clinical significance of red cell aggregation in the human subcutaneous vein using a high-frequency transducer (10 MHz): a preliminary report (Kitamura), 933

Chrisler, W. B., see Miller, D. L.

Christopher, D. A., Burns, P. N., Starkoski, B. G. and Foster, F. S.: a high-frequency pulsed-wave Doppler ultrasound system for the detection and imaging of blood flow in the microcirculation, 997

Christy, D. H., see Lanza, G. M.

Chronic hepatitis
clinical application of hepatic venous hemodynamics by Doppler ultrasonography in chronic liver disease (Hamato), 829
intra- and extrahepatic arterial resistances in chronic hepatitis and liver cirrhosis (Piscaglia), 675
phase shift of the hepatic vein flow velocity waveform in chronic liver disease: experimental and clinical studies (Hamato), 821

Chronic liver disease
clinical application of hepatic venous hemodynamics by Doppler ultrasonography in chronic liver disease (Hamato), 829
phase shift of the hepatic vein flow velocity waveform in chronic liver disease: experimental and clinical studies (Hamato), 821

Cirrhosis
clinical application of hepatic venous hemodynamics by Doppler ultrasonography in chronic liver disease (Hamato), 829
Doppler ultrasound in the evaluation of cirrhotic patients: the prevalence of intrahepatic arteriovenous shunting, and implications for diagnosis of hepatocellular carcinoma (Taylor), 1155

intra- and extrahepatic arterial resistances in chronic hepatitis and liver cirrhosis (Piscaglia), 675
phase shift of the hepatic vein flow velocity waveform in chronic liver disease: experimental and clinical studies (Hamato), 821
ultrasonic characterization of tissues *via* backscatter frequency dependence (Stetson), 989

Clarke, G. D., see Hatab, M. R.

Clarke, R. L. and ter Haar, G. R.: temperature rise recorded during lesion formation by high-intensity focused ultrasound, 299

Cleveland, R. O., McAteer, J. A., Andreoli, S. P. and Crum, L. A.: the effect of polypropylene vials on lithotripter shock waves, 939

Cloutier, G., see Fontaine, I.

Cloutier, G., Weng, X., Roederer, G. O., Allard, L., Tardif, F. and Beaulieu, R.: differences in the erythrocyte aggregation level between veins and arteries of normolipidemic and hyperlipidemic individuals, 1383

Coagulative necrosis
liver hemostasis using high-intensity focused ultrasound (Vaezy), 1413

Cobbold, R. S. C., see Bascom, P. A. J.

Coefficient of kurtosis
nonGaussian statistical property of the ultrasonic Doppler signal downstream of a severe stenosis (Fontaine), 41

Coleman, D. J., see Silverman, R. H.

Collagen synthesis
the stimulation of bone formation *in vitro* by therapeutic ultrasound (Reher), 1251

Color Doppler
a high-frequency pulsed-wave Doppler ultrasound system for the detection and imaging of blood flow in the microcirculation (Christopher), 997
an improved flow evaluation scheme in orifices of different aspect ratios (Anayiotos), 231
color flow mapping and hemodynamics (Beach), 319
color flow mapping (Ferrara), 321
colour velocity flow measurement: *in vitro* validation and application to human carotid (Deane), 447
Doppler ultrasound in the evaluation of cirrhotic patients: the prevalence of intrahepatic arteriovenous shunting, and implications for diagnosis of hepatocellular carcinoma (Taylor), 1155
insufficient and absent acoustic temporal bone window: potential and limitations of transcranial contrast-enhanced color-coded sonography and contrast-enhanced power-based sonography (Postert), 857
new signs of breast cancer: high resistance flow and variations in resistive indices evaluation by color Doppler sonography (Hollerweger), 851
peak velocity estimation in arterial stenosis models using colour vector Doppler (Hoskins), 889
preliminary results of power Doppler imaging in benign prostatic hyperplasia (Kojima), 1305
prognostic significance of color Doppler findings in head and neck tumors (Delorme), 1311

rapid measurement of the spatial resolution of colour flow scanners (Li), 591
the 3-D and 2-D color flow display of breast masses (Carson), 837
the reproducibility of color Doppler duplex sonography in the measurement of renal arterial blood velocity (Imuta), 813
thoraxsonography—part II: peripheral pulmonary consolidation (Mathis), 1141
ultrasonic color flow mapping: the visualization of four-dimensional cardiac and vascular flow phenomena using two dimensions and "real time" (Beach), 347

Color flow mapping
color flow mapping and hemodynamics (Beach), 319
color flow mapping (Ferrara), 321
colour velocity flow measurement: *in vitro* validation and application to human carotid (Deane), 447
effects of velocity distribution, diameter measurement and velocity tracing on the accuracy of cardiac output measurement by pulsed Doppler echocardiography in the aortic annulus of pigs (Zhou), 177
peak velocity estimation in arterial stenosis models using colour vector Doppler (Hoskins), 889
rapid measurement of the spatial resolution of colour flow scanners (Li), 591
ultrasonic color flow mapping: the visualization of four-dimensional cardiac and vascular flow phenomena using two dimensions and "real time" (Beach), 347
ultrasound Doppler vector tomography measurements of directional blood flow (Jansson), 47

Color vector Doppler
peak velocity estimation in arterial stenosis models using colour vector Doppler (Hoskins), 889
ultrasound Doppler vector tomography measurements of directional blood flow (Jansson), 47

Color velocity mapping
colour velocity flow measurement: *in vitro* validation and application to human carotid (Deane), 447
peak velocity estimation in arterial stenosis models using colour vector Doppler (Hoskins), 889
ultrasound Doppler vector tomography measurements of directional blood flow (Jansson), 47

Comess, K. A., see Beach, K. W.

Compact bone
a novel method to measure acoustic speed of bone tissue (Chen), 1337
bone status after long-term anticonvulsant therapy in epileptic patients: evaluation using quantitative ultrasound of calcaneus and phalanges (Pluskiewicz), 553
measurement of velocity and attenuation of shear waves in bovine compact bone using ultrasonic spectroscopy (Wu), 129

Complex cross-correlation
a radiofrequency domain complex cross-correlation model to estimate blood flow velocity and tissue motion by means of ultrasound (Brands), 911

Compliance
variation of common carotid artery elasticity with intimal-medial thickness: the ARIC study (Riley), 157

Connors, B. A., see Lifshitz, D. A.

Contractility
effect of ultrasound on the contraction of isolated myocardial cells of adult rats (Salz), 143

Contrast
characterization of echographic image texture by co-occurrence matrix parameters (Valckx), 559
direct effects of DC cardioversion on blood echogenicity: an *in vitro* study (Fatkin), 135
phantoms and automated system for testing the resolution of ultrasound scanners (Rownd), 245

Contrast agent
color flow mapping (Ferrara), 321
contrast ultrasonography for 2-D opacification of heart cavities, peripheral vessels, kidney and muscle (Strauss), 975
correlation of ultrasound-induced hemolysis with cavitation detector output *in vitro* (Everbach), 619
gray-scale second harmonic imaging of the liver: a preliminary animal study (Kono), 719
hemolysis *in vivo* from exposure to pulsed ultrasound (Dalecki), 315
high-frequency ultrasonic detection of thrombi with a targeted contrast system (Lanza), 863
insufficient and absent acoustic temporal bone window: potential and limitations of transcranial contrast-enhanced color-coded sonography and contrast-enhanced power-based sonography (Postert), 857
preliminary study in differential contrast echography (Arditi), 1185
quantitative acoustic characterization of a new surfactant-based ultrasound contrast agent (Forsberg), 1201
remnants of Albunex nucleate acoustic cavitation (Dalecki), 1405
second harmonic characteristics of the ultrasound contrast agents Albunex and FSO69 (Krishna), 453
the influence of contrast agents on hemorrhage produced by lithotripter fields (Dalecki), 1435
transfection of a reporter plasmid into cultured cells by sonoporation *in vitro* (Bao), 953
ultrasonically induced hemolysis at high cell and gas body concentrations in a thin-disc exposure chamber (Miller), 625
ultrasound contrast agent in intravascular echography: an *in vitro* study (Cachard), 705
ultrasound contrast media and their use in obstetrics and gynecology (Abramowicz), 1287

Co-occurrence matrix
characterization of echographic image texture by co-occurrence matrix parameters (Valckx), 559

Cord compression
umbilical venous pulsation and regional circulatory disturbance (Nakai), 1165

Coronary artery
characterisation of atherosclerotic plaque by spectral analysis of intravascular ultrasound: an *in vitro* methodology (Spencer), 191

Cortiocotherapy
quantitative ultrasound of the heel and serum and urinary cortisol values in assessment of long-term corticotherapy side effects in female bronchial asthma patients (Kos-Kudla), 1325

Costa, F., see Anayiotos, A. S.

Cow
a novel method to measure acoustic speed of bone tissue (Chen), 1337
measurement of velocity and attenuation of shear waves in bovine compact bone using ultrasonic spectroscopy (Wu), 129

Cox, C., see Brayman, A. A.

Cox, C., see Dalecki, D.

Craig, D. M., see Ota, T.

Cross-correlation
the nonstationary strain filter in elastography: Part I. frequency-dependent attenuation (Varghese), 1343
the nonstationary strain filter in elastography: Part II. lateral and elevational decorrelation (Kallel), 1357

Crum, L. A., see Cleveland, R. O.

Crum, L., see Vaezy, S.

Cubberley, F., see Wu, J.

Curl
ultrasound Doppler vector tomography measurements of directional blood flow (Jansson), 47

Cutaneous radiation syndrome
sonographic determination of cutaneous and subcutaneous fibrosis after accidental exposure to ionising radiation in the course of the Chernobyl nuclear power plant accident (Gottlöber), 9

Cyclic variation
influence of data processing on cyclic variation of integrated backscatter and wall thickness in stunned porcine myocardium (van der Steen), 405
influences of ultrasonic machine settings, transducer frequency and placement of region of interest on the measurement of integrated backscatter and cyclic variation (Ota), 1059

Cytoxoticity
mechanism of ultrasound-enhanced porphyrin cytotoxicity. Part I: a search for free radical effects (Worthington), 1095

Czarnota, G. J., Kolios, M. C., Vaziri, H., Benchimol, S., Ottensmeyer, F. P., Sherar, M. D. and Hunt, J. W.: ultrasonic biomicroscopy of viable, dead and apoptotic cells, 961

D

Dalecki, D., Child, S. Z., Raeman, C. H., Cox, C. and Carstensen, E. L.: ultrasonically induced lung hemorrhage in young swine, 777

Dalecki, D., Child, S. Z., Raeman, C. H., Cox, C., Penney, D. P. and Carstensen, E. L.: age dependence of ultrasonically induced lung hemorrhage in mice, 767

Dalecki, D., Child, S. Z., Raeman, C. H., Penney, D. P., Mayer, R., Cox, C. and Carstensen, E. L.: thresholds for fetal hemorrhages produced by a piezoelectric lithotripter, 287

Dalecki, D., Raeman, C. H., Child, S. Z., Cox, C., Francis, C. W., Meltzer, R. S. and Carstensen, E. L.: hemolysis *in vivo* from exposure to pulsed ultrasound, 315

Dalecki, D., Raeman, C. H., Child, S. Z., Penney, D. P. and Carstensen, E. L.: remnants of Albunex nucleate acoustic cavitation, 1405

Dalecki, D., Raeman, C. H., Child, S. Z., Penney, D. P., Mayer, R. and Carstensen, E. L.: the influence of contrast agents on hemorrhage produced by Lithotripter Fields, 1435

Dalecki, D., Raeman, C. H., Child, S. Z. and Carstensen, E. L.: effects of pulsed ultrasound on the frog heart: III. the radiation force mechanism, 275

Dalecki, D., see MacRobbie, A. G.

Dawes, L.: manual of obstetric and gynaecologic ultrasound, 1441

Dawes, L.: pocket atlas of obstetric ultrasound, 1442

De Korte, C. L., Céspedes, E. I., van der Steen, A. F. W. and Lancée, C. T.: intravascular elasticity imaging using ultrasound: feasibility studies in phantom, 735

Deane, C. R. and Markus, H. S.: colour velocity flow measurement: *in vitro* validation and application to human carotid, 447

DeAngelis, G., see Ferrara, K.

DeCarvalho, C. T., see Anayiotos, A. S.

Decay constant
decay constant of Doppler flow waveform as a possible indicator of ovarian malignancy (Tepper), 1171

Deconvolution
deconvolution process in measurement of arterial velocity profiles *via* an ultrasonic pulsed Doppler velocimeter for evaluation of the wall shear rate (Flaud), 425

Decorrelation
on the use of envelope and RF signal decorrelation as tissue strain estimators (Alam), 1427

Degassing
quantitation of shock-wave cavitation damage *in vitro* (Lifshitz), 461

Delius, M.: minimal static excess pressure minimises the effect of extracorporeal shock waves on cells and reduces it on gallstones, 611

Delorme, S., Dietz, A., Rudat, V., Zuna, I., Bahner, M. L. and van Kaick, G.: prognostic significance of color Doppler findings in head and neck tumors, 1311

Denaturation flow field
temperature rise recorded during lesion formation by high-intensity focused ultrasound (Clarke), 299

Deskilling
automatic attenuation compensation for ultrasonic imaging (Hughes), 651
interactive automatic fetal head measurements from ultrasound images using multimedia computer technology (Pathak), 665

Detectability
phantoms and automated system for testing the resolution of ultrasound scanners (Rownd), 245

Detmer, P. R., see Leotta, D. F.

Diastolic function
echo machine-imposed limit on transmitral spectral Doppler velocity-profile analysis (Hall), 1225

Dietz, A., see Delorme, S.

Differential contrast echography
preliminary study in differential contrast echography (Arditi), 1185

Differential imaging
preliminary study in differential contrast echography (Arditi), 1185

Dillon, S. M., see Ren, J-F.

Distensibility
comparison of B-mode, M-mode and echo-tracking methods for measurement of the arterial distension waveform (Stadler), 879
stiffness and diameter of the common carotid artery and abdominal aorta in women (Ahlgren), 983
variation of common carotid artery elasticity with intimal-medial thickness: the ARIC study (Riley), 157

Do, D-D., Chatterjee, T. and Mahler, F.: unusual pseudoaneurysms after catheterization: successful treatment by ultrasound-guided compression, 377

Dog
temperature rise recorded during lesion formation by high-intensity focused ultrasound (Clarke), 299
ultrasound attenuation and backscatter in the liver during prednisone administration (Lu), 1

Dong, F., see Rownd, J. J.

Doppler
a high-frequency pulsed-wave Doppler ultrasound system for the detection and imaging of blood flow in the microcirculation (Christopher), 997
a radiofrequency domain complex cross-correlation model to estimate

blood flow velocity and tissue motion by means of ultrasound (Brands), 911
a study of the spectral broadening of simulated Doppler signals using FFT and AR modelling (Keeton), 1033
acoustic streaming: comparison of low-amplitude linear model with streaming velocities measured by 32-MHz Doppler (Nowicki), 783
an FFT-based flow profiler for high-resolution *in vivo* investigations (Tortoli), 899
analysis of the frequency modulation present in Doppler ultrasound signals may allow differentiation between particulate and gaseous cerebral emboli (Smith), 727
assessment of mitral A-wave transit time to cardiac outflow tract and isovolumic relaxation time of left ventricle in the appropriate and small-for–gestational–age human fetus (Tsyvian), 187
clinical application of hepatic venous hemodynamics by Doppler ultrasonography in chronic liver disease (Hamato), 829
color flow mapping (Ferrara), 321
critical comparison of indices and threshold values for assessing placenta performance using Doppler ultrasound (Joern), 1179
decay constant of Doppler flow waveform as a possible indicator of ovarian malignancy (Tepper), 1171
deconvolution process in measurement of arterial velocity profiles *via* an ultrasonic pulsed Doppler velocimeter for evaluation of the wall shear rate (Flaud), 425
differences in the erythrocyte aggregation level between veins and arteries of normolipidemic and hyperlipidemic individuals (Cloutier), 1383
Doppler myocardial imaging vs. B-mode grey-scale imaging: a comparative *in vitro* and *in vivo* study into their relative efficacy in endocardial boundary detection (Lange), 69
Doppler sensors and harnesses for cardiac and peripheral arterial flow monitoring (Arbeille), 415
Doppler ultrasound in the evaluation of cirrhotic patients: the prevalence of intrahepatic arteriovenous shunting, and implications for diagnosis of hepatocellular carcinoma (Taylor), 1155
ductus venosus revisited: a Doppler blood flow evaluation in the first trimester of pregnancy (Montenegro), 171
echo machine-imposed limit on transmitral spectral Doppler velocity-profile analysis (Hall), 1225
effects of velocity distribution, diameter measurement and velocity tracing on the accuracy of cardiac output measurement by pulsed Doppler echocardiography in the aortic annulus of pigs (Zhou), 177
estimation of axial blood velocity using the Doppler equation corrected for broadening (Chabria), 967
evaluation of cerebral arterial flow with transcranial Doppler ultrasound: theoretical development and phantom studies (Hatab), 1025
feasibility of angle-independent Doppler color imaging for *in vivo* application: preliminary study on carotid arteries (Fei), 59
intra- and extrahepatic arterial resistances in chronic hepatitis and liver cirrhosis (Piscaglia), 675
intraoperative evaluation of small-calibre arterial reconstructions (Sugawara), 473
neural network analysis of Doppler ultrasound blood flow signals: a pilot study (Wright), 683

new signs of breast cancer: high resistance flow and variations in resistive indices evaluation by color Doppler sonography (Hollerweger), 851
nonGaussian statistical property of the ultrasonic Doppler signal downstream of a severe stenosis (Fontaine), 41
ophthalmic artery aneurysms: an investigation by duplex scan (Molnar), 1319
peak velocity estimation in arterial stenosis models using colour vector Doppler (Hoskins), 889
phase shift of the hepatic vein flow velocity waveform in chronic liver disease: experimental and clinical studies (Hamato), 821
preliminary results of power Doppler imaging in benign prostatic hyperplasia (Kojima), 1305
prognostic significance of color Doppler findings in head and neck tumors (Delorme), 1311
quantitative acoustic characterization of a new surfactant-based ultrasound contrast agent (Forsberg), 1201
rapid measurement of the spatial resolution of colour flow scanners (Li), 591
relation of the flow field distal to a moderate stenosis to the Doppler power (Bascom), 25
signals from dual gated TCD systems: curious observations and possible explanations (Smith), 15
the 3-D and 2-D color flow display of breast masses (Carson), 837
thoraxsonography—part II: peripheral pulmonary consolidation (Mathis), 1141
ultrasonic color flow mapping: the visualization of four-dimensional cardiac and vascular flow phenomena using two dimensions and "real time" (Beach), 347
ultrasound Doppler vector tomography measurements of directional blood flow (Jansson), 47
ultrasound in ophthalmology (Fledelius), 365
umbilical venous pulsation and regional circulatory disturbance (Nakai), 1165

Doppler color flow mapping

color flow mapping (Ferrara), 321
color flow mapping and hemodynamics (Beach), 319
colour velocity flow measurement: *in vitro* validation and application to human carotid (Deane), 447
effects of velocity distribution, diameter measurement and velocity tracing on the accuracy of cardiac output measurement by pulsed Doppler echocardiography in the aortic annulus of pigs (Zhou), 177
feasibility of angle-independent Doppler color imaging for *in vivo* application: preliminary study on carotid arteries (Fei), 59
peak velocity estimation in arterial stenosis models using colour vector Doppler (Hoskins), 889
rapid measurement of the spatial resolution of colour flow scanners (Li), 591
ultrasonic color flow mapping: the visualization of four-dimensional cardiac and vascular flow phenomena using two dimensions and "real time" (Beach), 347
ultrasound Doppler vector tomography measurements of directional blood flow (Jansson), 47

Doppler indices
critical comparison of indices and threshold values for assessing placenta performance using Doppler ultrasound (Joern), 1179

Doppler myocardial imaging
Doppler myocardial imaging vs. B-mode grey-scale imaging: a comparative *in vitro* and *in vivo* study into their relative efficacy in endocardial boundary detection (Lange), 69

Doppler power
relation of the flow field distal to a moderate stenosis to the Doppler power (Bascom), 25

Dose
in vitro study of the mechanical effects of shock-wave lithotripsy (Howard), 1107

Dose response
quantitative acoustic characterization of a new surfactant-based ultrasound contrast agent (Forsberg), 1201

Dost, P. and Kaiser, S.: ultrasonographic biometry in salivary glands, 1299

Doukas, A. G., see Lee, S.

DSP
an FFT-based flow profiler for high-resolution *in vivo* investigations (Tortoli), 899

Duck, F. A., see Hughes, D. I.

Ductus venosus
ductus venosus revisited: a Doppler blood flow evaluation in the first trimester of pregnancy (Montenegro), 171

Dunmire, B., see Beach, K. W.

Dunn, F., see Saijo, Y.

E

Early pregnancy
ductus venosus revisited: a Doppler blood flow evaluation in the first trimester of pregnancy (Montenegro), 171

Echo tracking
comparison of B-mode, M-mode and echo-tracking methods for measurement of the arterial distension waveform (Stadler), 879

Echocardiography
an improved flow evaluation scheme in orifices of different aspect ratios (Anayiotos), 231
characterisation of red and white thrombus by intravascular ultrasound using radiofrequency and videodensitometric data-based texture analysis (Ramo), 1195
direct effects of DC cardioversion on blood echogenicity: an *in vitro* study (Fatkin), 135
Doppler myocardial imaging vs. B-mode grey-scale imaging: a comparative

in vitro and *in vivo* study into their relative efficacy in endocardial boundary detection (Lange), 69
echo machine-imposed limit on transmitral spectral Doppler velocity-profile analysis (Hall), 1225
effects of velocity distribution, diameter measurement and velocity tracing on the accuracy of cardiac output measurement by pulsed Doppler echocardiography in the aortic annulus of pigs (Zhou), 177
high-frequency ultrasonic detection of thrombi with a targeted contrast system (Lanza), 863
lower frequency (5 MHz) intracardiac echocardiography in a large swine model: imaging views and research applications (Ren), 871

Echogenicity
detection and clinical significance of red cell aggregation in the human subcutaneous vein using a high-frequency transducer (10 MHz): a preliminary report (Kitamura), 933

Echo-tracking
stiffness and diameter of the common carotid artery and abdominal aorta in women (Ahlgren), 983
variation of common carotid artery elasticity with intimal-medial thickness: the ARIC study (Riley), 157

Effusion volume
thoraxsonography—part I: chest wall and pleura (Mathis), 1131

Elastic modulus
variation of common carotid artery elasticity with intimal-medial thickness: the ARIC study (Riley), 157

Elasticity
automated detection of local artery wall thickness based on M-line signal processing (Hoeks), 1017
measurement of shear-wave velocity by ultrasound critical-angle reflectometry (UCR) (Mehta), 1123
on the use of envelope and RF signal decorrelation as tissue strain estimators (Alam), 1427
tissue-equivalent vessel phantoms for intravascular ultrasound (Ryan), 261
variation of common carotid artery elasticity with intimal-medial thickness: the ARIC study (Riley), 157

Elastogram
the nonstationary strain filter in elastography: Part I. frequency-dependent attenuation (Varghese), 1343
the nonstationary strain filter in elastography: Part II. lateral and elevational decorrelation (Kallel), 1357

Elastography
intravascular elasticity imaging using ultrasound: feasibility studies in phantoms (De Korte), 735
on the use of envelope and RF signal decorrelation as tissue strain estimators (Alam), 1427
reduction of signal decorrelation from mechanical compression of tissues by temporal stretching: applications to elastography (Alam), 95

the nonstationary strain filter in elastography: Part I. frequency-dependent attenuation (Varghese), 1343
the nonstationary strain filter in elastography: Part II. lateral and elevational decorrelation (Kallel), 1357

Elbeshir, E-N. I., see Reher, P.

Electronic focusing
a piezocomposite shock-wave generator with electronic focusing capability: application for producing cavitation-induced lesions in rabbit liver (Tavakkoli), 107

El-Fallah, A. I., Plantec, M. B. and Ferrara, K. W.: ultrasonic measurement of breast tissue motion and the implications for velocity estimation, 1047

Eliott, M. R., see Thrush, A. J.

Elmahdi, A. M., see Anayiotos, A. S.

Embolism
analysis of the frequency modulation present in Doppler ultrasound signals may allow differentiation between particulate and gaseous cerebral emboli (Smith), 727
signals from dual-gated TCD systems: curious observations and possible explanations (Smith), 15
thoraxsonography—part II: peripheral pulmonary consolidation (Mathis), 1141

Endocardial boundary detection
Doppler myocardial imaging vs. B-mode grey-scale imaging: a comparative *in vitro* and *in vivo* study into their relative efficacy in endocardial boundary detection (Lange), 69

Endometrial biopsy
lack of correlation between ultrasonography and histologic staging of the endometrium in *in vitro* fertilization (IVF) patients (Sterzik), 165

Endometrium
lack of correlation between ultrasonography and histologic staging of the endometrium in *in vitro* fertilization (IVF) patients (Sterzik), 165

Enhancement
quantitative acoustic characterization of a new surfactant-based ultrasound contrast agent (Forsberg), 1201

Entropy
characterization of echographic image texture by cooccurrence matrix parameters (Valckx), 559

Epilepsy
bone status after long-term anticonvulsant therapy in epileptic patients: evaluation using quantitative ultrasound of calcaneus and phalanges (Pluskiewicz), 553

Equipment performance
an experimental study of the reflection from spherical and flat-ended cylindrical targets suitable for fetal Doppler performance assessment (Preston), 117

Eriksson, R., see Jansson, T.

Errors
a radiofrequency domain complex cross-correlation model to estimate blood flow velocity and tissue motion by means of ultrasound (Brands), 911
a study of the quantitative and qualitative impact of catheter shaft angulation in a mechanical intravascular ultrasound system (Kearney), 87
an evaluation of the potential and limitations of three-dimensional reconstructions from intravascular ultrasound images (Thrush), 437
colour velocity flow measurement: *in vitro* validation and application to human carotid (Deane), 447
electromagnetic hydrophone for pressure determination of shock-wave pulses (Etienne), 747
influence of tissue-preservation methods on arterial geometry and echogenicity (Wilhjelm), 1071
on the use of envelope and RF signal decorrelation as tissue strain estimators (Alam), 1427
performance of a miniature magnetic position sensor for three-dimensional ultrasound imaging (Leotta), 597
reduction of signal decorrelation from mechanical compression of tissues by temporal stretching: applications to elastography (Alam), 95
reproducibility of shear rate and shear stress assessment by means of ultrasound in the common carotid artery of young human males and females (Samijo), 583
the effect of polypropylene vials on lithotripter shock waves (Cleveland), 939
the reproducibility of color Doppler duplex sonography in the measurement of renal arterial blood velocity (Imuta), 813
ultrasonographic biometry in salivary glands (Dost), 1299

Erythrocyte
comparative sensitivity of human erythrocytes and lymphocytes to sonolysis by 1-MHz ultrasound (Miller), 635
detection and clinical significance of red cell aggregation in the human subcutaneous vein using a high-frequency transducer (10 MHz): a preliminary report (Kitamura), 933
differences in the erythrocyte aggregation level between veins and arteries of normolipidemic and hyperlipidemic individuals (Cloutier), 1383
hemolysis of 40% hematocrit, Albunex-supplemented human erythrocytes by pulsed ultrasound: frequency, acoustic pressure and pulse length dependence (Brayman), 1237
nonGaussian statistical property of the ultrasonic Doppler signal downstream of a severe stenosis (Fontaine), 41
stress-wave induced membrane permeation of red blood cells is facilitated by aquaporins (Lee), 1089

ESWL
electromagnetic hydrophone for pressure determination of shock-wave pulses (Etienne), 747
in vitro study of the mechanical effects of shock-wave lithotripsy (Howard), 1107
minimal static excess pressure minimises the effect of extracorporeal shock waves on cells and reduces it on gallstones (Delius), 611
quantitation of shock-wave cavitation damage *in vitro* (Lifshitz), 461

remnants of Albunex nucleate acoustic cavitation (Dalecki), 1405
shock-wave measurement using a calibrated interferometric fiber-tip sensor (Koch), 1259
stress-wave–induced membrane permeation of red blood cells is facilitated by aquaporins (Lee), 1089
the effect of polypropylene vials on lithotripter shock waves (Cleveland), 939
the influence of contrast agents on hemorrhage produced by lithotripter fields (Dalecki), 1435
thresholds for fetal hemorrhages produced by a piezoelectric lithotripter (Dalecki), 287

Etani, H., see Imuta, N.

Etienne, J., Filipczynski, L., Kujawska, T. and Zienkiewicz, B.: electromagnetic hydrophone for pressure determination of shock-wave pulses, 747

Evan, A. P., see Lifshitz, D. A.

Evans, D. H., see Keeton, P. I. J.

Evans, D. H., see Smith, J. L.

Evans, D. H., see Thrush, A. J.

Evans, G. W., see Riley, W. A.

Everbach, E. C., Makin, I., Raj, S., Azadniv, M. and Meltzer, R. S.: correlation of ultrasound-induced hemolysis with cavitation detector output *in vitro*, 619

Ex vivo *irradiation*
temperature rise recorded during lesion formation by high-intensity focused ultrasound (Clarke), 299

Extracellular matrix
correlation of ultrasound parameter imaging with microcirculatory patterns in uveal melanomas (Silverman), 573

Extracorporeal shock waves
in vitro study of the mechanical effects of shock-wave lithotripsy (Howard), 1107
minimal static excess pressure minimises the effect of extracorporeal shock waves on cells and reduces it on gallstones (Delius), 611

Eyal, S., see Tepper, R.

Eye
correlation of ultrasound parameter imaging with microcirculatory patterns in uveal melanomas (Silverman), 573

F

Faerestrand, S., see Zhou, Y-Q.

False aneurysm
unusual pseudoaneurysms after catheterization: successful treatment by ultrasound-guided compression (Do), 377

Fatkin, D., Loupas, T. and Feneley, M. P.: direct effects of DC cardioversion on blood echogenicity: an *in vitro* study, 135

Favaretto, A. L. V., see Haddad, S.

Federlein, J., see Postert, T.

Fei, D-Y., Liu, D. D., Fu, C-T., Makhoul, R. G. and Fisher, M. R.: feasibility of angle-independent Doppler color imaging for *in vivo* application: preliminary study on carotid arteries, 59

Feleppa, E. J., see Lizzi, F. L.

Feleppa, E. J., see Noritomi, T.

Femoral
neural network analysis of Doppler ultrasound blood flow signals: a pilot study (Wright), 683

Feneley, M. P., see Fatkin, D.

Fenn, L. N., see Lange, A.

Fernandez, R., see Martin, K.

Ferrara, K. and DeAngelis, G.: colour flow mapping, 321

Ferrara, K. W., see El-Fallah, A. I.

Fetal
an experimental study of the reflection from spherical and flat-ended cylindrical targets suitable for fetal Doppler performance assessment (Preston), 117
assessment of mitral A-wave transit time to cardiac outflow tract and isovolumic relaxation time of left ventricle in the appropriate and small-for–gestational–age human fetus (Tsyvian), 187
interactive automatic fetal head measurements from ultrasound images using multimedia computer technology (Pathak), 665
three-dimensional ultrasound assessment of fetal liver volume in normal pregnancy: a comparison of reproducibility with two-dimensional ultrasound and a search for a volume constant (Chang), 381
thresholds for fetal hemorrhages produced by a piezoelectric lithotripter (Dalecki), 287
umbilical venous pulsation and regional circulatory disturbance (Nakai), 1165

Fetal Doppler
an experimental study of the reflection from spherical and flat-ended cylindrical targets suitable for fetal Doppler performance assessment (Preston), 117

Fetal flow
umbilical venous pulsation and regional circulatory disturbance (Nakai), 1165

Fetal growth
three-dimensional ultrasound assessment of fetal liver volume in normal pregnancy: a comparison of reproducibility with two-dimensional ultrasound and a search for a volume constant (Chang), 381

Fetal growth and development
interactive automatic fetal head measurements from ultrasound images using multimedia computer technology (Pathak), 665

Fetal head measurement
interactive automatic fetal head measurements from ultrasound images using multimedia computer technology (Pathak), 665

Fetal liver volume
three-dimensional ultrasound assessment of fetal liver volume in normal pregnancy: a comparison of reproducibility with two-dimensional ultrasound and a search for a volume constant (Chang), 381

Fetal lung
thresholds for fetal hemorrhages produced by a piezoelectric lithotripter (Dalecki), 287

FFT
a study of the spectral broadening of simulated Doppler signals using FFT and AR modelling (Keeton), 1033
an FFT-based flow profiler for high-resolution *in vivo* investigations (Tortoli), 899

Fiberoptic sensors
shock-wave measurement using a calibrated interferometric fiber-tip sensor (Koch), 1259

Fibrin
high-frequency ultrasonic detection of thrombi with a targeted contrast system (Lanza), 863

Fibrinogen
detection and clinical significance of red cell aggregation in the human subcutaneous vein using a high-frequency transducer (10 MHz): a preliminary report (Kitamura), 933

Fibrosis
sonographic determination of cutaneous and subcutaneous fibrosis after accidental exposure to ionising radiation in the course of the Chernobyl nuclear power plant accident (Gottlöber), 9

Filipczynski, L., see Etienne, J.

Finet, G., see Cachard, C.

Finite amplitude effects
a numerical study of the effect of drive level on the intensity loss from an ultrasonic beam (Baker), 1083

Finite element modeling
an improved flow evaluation scheme in orifices of different aspect ratios (Anayiotos), 231

Fischer, S. E., see Lanza, G. M.

Fisher, M. R., see Fei, D-Y.

Flaud, P., Bensalah, A. and Peronneau, P.: deconvolution process in measurement of arterial velocity profiles *via* an ultrasonic pulsed Doppler velocimeter for evaluation of the wall shear rate, 425

Fledelius, H. C.: ultrasound in ophthalmology, 365

Flute, T. J., see Lee, S.

Flow
a radiofrequency domain complex cross-correlation model to estimate blood flow velocity and tissue motion by means of ultrasound (Brands), 911
color flow mapping (Ferrara), 321
colour velocity flow measurement: *in vitro* validation and application to human carotid (Deane), 447
contrast ultrasonography for 2-D opacification of heart cavities, peripheral vessels, kidney and muscle (Strauss), 975
critical comparison of indices and threshold values for assessing placenta performance using Doppler ultrasound (Joern), 1179
decay constant of Doppler flow waveform as a possible indicator of ovarian malignancy (Tepper), 1171
deconvolution process in measurement of arterial velocity profiles *via* an ultrasonic pulsed Doppler velocimeter for evaluation of the wall shear rate (Flaud), 425
differences in the erythrocyte aggregation level between veins and arteries of normolipidemic and hyperlipidemic individuals (Cloutier), 1383
Doppler sensors and harnesses for cardiac and peripheral arterial flow monitoring (Arbeille), 415
ductus venosus revisited: a Doppler blood flow evaluation in the first trimester of pregnancy (Montenegro), 171
echo machine-imposed limit on transmitral spectral Doppler velocity-profile analysis (Hall), 1225
evaluation of cerebral arterial flow with transcranial Doppler ultrasound: theoretical development and phantom studies (Hatab), 1025
gray-scale second harmonic imaging of the liver: a preliminary animal study (Kono), 719
neural network analysis of Doppler ultrasound blood flow signals: a pilot study (Wright), 683
new signs of breast cancer: high resistance flow and variations in resistive indices evaluation by color Doppler sonography (Hollerweger), 851
nonGaussian statistical property of the ultrasonic Doppler signal downstream of a severe stenosis (Fontaine), 41
ophthalmic artery aneurysms: an investigation by duplex scan (Molnar), 1319
peak velocity estimation in arterial stenosis models using colour vector Doppler (Hoskins), 889
rapid measurement of the spatial resolution of colour flow scanners (Li), 591
reproducibility of shear rate and shear stress assessment by means of ultrasound in the common carotid artery of young human males and females (Samijo), 583
the 3-D and 2-D color flow display of breast masses (Carson), 837
the reproducibility of color Doppler duplex sonography in the measurement of renal arterial blood velocity (Imuta), 813
ultrasonic color flow mapping: the visualization of four-dimensional cardiac and vascular flow phenomena using two dimensions and "real time" (Beach), 347
ultrasound Doppler vector tomography measurements of directional blood flow (Jansson), 47

Flow discrimination
color flow mapping (Ferrara), 321

Flow field
an improved flow evaluation scheme in orifices of different aspect ratios (Anayiotos), 231

Flow index
evaluation of cerebral arterial flow with transcranial Doppler ultrasound: theoretical development and phantom studies (Hatab), 1025

Flow profile
an improved flow evaluation scheme in orifices of different aspect ratios (Anayiotos), 231
effects of velocity distribution, diameter measurement and velocity tracing on the accuracy of cardiac output measurement by pulsed Doppler echocardiography in the aortic annulus of pigs (Zhou), 177
neural network analysis of Doppler ultrasound blood flow signals: a pilot study (Wright), 683
relation of the flow field distal to a moderate stenosis to the Doppler power (Bascom), 25

Flow velocity
a radiofrequency domain complex cross-correlation model to estimate blood flow velocity and tissue motion by means of ultrasound (Brands), 911

Flow visualization
relation of the flow field distal to a moderate stenosis to the Doppler power (Bascom), 25

Flow waveform
decay constant of Doppler flow waveform as a possible indicator of ovarian malignancy (Tepper), 1171

Focusing
in vitro study of the mechanical effects of shock-wave lithotripsy (Howard), 1107
the effect of polypropylene vials on lithotripter shock waves (Cleveland), 939

Folberg, R., see Silverman, R. H.

Fontaine, I., Cloutier, G. and Allard, L.: nonGaussian statistical property of the ultrasonic Doppler signal downstream of a severe stenosis, 41

Forleo, P., see Marinoni, M.

Fornès, P., see Bridal, S. L.

Forsberg, F., Wu, Y., Makin, I. R. S., Wang, W. and Wheatley, M. A.: quantitative acoustic characterization of a new surfactant-based ultrasound contrast agent, 1201

Fort, A., Manfredi, C. and Rocchi, S.: recursive autoregressive spectral maps for ocular pathology detection, 391

Foster, F. S., see Christopher, D. A.

Foster, F. S., see Ryan, L. K.

Fowlkes, J. B., see Carson, P. L.

Fox, K. A. A., see Lange, A.

Fox, K. A. A., see Ramo, M. P.

Fox, K. A. A., see Spencer, T.

Fracture healing
the stimulation of bone formation *in vitro* by therapeutic ultrasound (Reher), 1251

Francis, C. W., see Dalecki, D.

Francon, D., see Cachard, C.

Frank, G. R., see Rownd, J. J.

Free radicals
mechanism of ultrasound-enhanced porphyrin cytotoxicity. Part I: a search for free radical effects (Worthington), 1095

Frequency dependence
hemolysis of 40% hematocrit, Albunex-supplemented human erythrocytes by pulsed ultrasound: frequency, acoustic pressure and pulse length dependence (Brayman), 1237
the nonstationary strain filter in elastography: Part I. frequency-dependent attenuation (Varghese), 1343
the nonstationary strain filter in elastography: Part II. lateral and elevational decorrelation (Kallel), 1357
ultrasonic characterization of tissues *via* backscatter frequency dependence (Stetson), 989

Fu, C-T., see Fei, D-Y.

G

Gaffey, P. J., see Lanza, G. M.

Gagsteiger, F., see Sterzik, K.

Gahtan, V., see Noritomi, T.

Gaiani, S., see Piscaglia, F.

Gallstones
minimal static excess pressure minimises the effect of extracorporeal shock waves on cells and reduces it on gallstones (Delius), 611

Garcia-Tsao, G., see Taylor, C. R.

Gas bodies
acoustic cavitation nuclei survive the apparent ultrasonic destruction of Albunex microspheres (Brayman), 793

Gender
quantitative ultrasound of the heel and serum and urinary cortisol values in assessment of long-term corticotherapy side effects in female bronchial asthma patients (Kos-Kudla), 1325
reproducibility of shear rate and shear stress assessment by means of ultrasound in the common carotid artery of young human males and females (Samijo), 583
stiffness and diameter of the common carotid artery and abdominal aorta in women (Ahlgren), 983
the assessment of development of bone mass in children by quantitative ultrasound through the proximal phalanxes of the hand (Halaba), 1331

Gene therapy
transfection of a reporter plasmid into cultured cells by sonoporation *in vitro* (Bao), 953

Gene transfection
transfection of a reporter plasmid into cultured cells by sonoporation *in vitro* (Bao), 953

Geometric distortion
a study of the quantitative and qualitative impact of catheter shaft angulation in a mechanical intravascular ultrasound system (Kearney), 87

Germinal epithelium
ultrasound stimulation of rat testes damaged by Busulfan (Haddad), 1421

Gertner, M. R., Wilson, B. C. and Sherar, M. D.: ultrasound properties of liver tissue during heating, 1395

Gestational age
interactive automatic fetal head measurements from ultrasound images using multimedia computer technology (Pathak), 665

Gies, R. A., see Miller, D. L.

Giller, C. A., see Hatab, M. R.

Gimenez, G., see Cachard, C.

Ginanneschi, A., see Marinoni, M.

Goddard, D. A.: teaching atlas of breast ultrasound, 1441

Göttlober, P., Kerscher, M. J., Korting, H. C. and Peter, R. U.: sonographic determination of cutaneous and subcutaneous fibrosis after accidental exposure to ionising radiation in the course of the Chernobyl nuclear power plant accident, 9

Gough, N. A. J., see Wright, I. A.

Govil, A., see Carson, P. L.

Grab, D., see Sterzik, K.

Gramantieri, L., see Piscaglia, F.

Gritzmann, N., see Hollerweger, A.

Guided biopsy
lack of correlation between ultrasonography and histologic staging of the endometrium in *in vitro* fertilization (IVF) patients (Sterzik), 165
thoraxsonography—part II: peripheral pulmonary consolidation (Mathis), 1141
unusual pseudoaneurysms after catheterization: successful treatment by ultrasound-guided compression (Do), 377

Guidi, F., see Tortoli, T.

Guidi, G., see Tortoli, T.

Gynecology
the history of ultrasound in gynecology 1950–1980 (Levi), 481

H

ter Haar, G. R., see Barnett, S. B.

ter Haar, G. R., see Clarke, R. L.

ter Haar, G. R., see Chen, L.

Haddad, S., Carvalho, T. L. L., Anselmo-Franci, J. A., Petenusci, S. O. and Favaretto, A. L. V.: ultrasound stimulation of rat testes damaged by Busulfan, 1421

Halaba, Z. and Pluskiewicz, W.: the assessment of development of bone mass in children by quantitative ultrasound through the proximal phalanxes of the hand, 1331

Hall, A. F., Bettlach, J., Nudelman, S. P. and Kovács, S. J.: echo machine-imposed limit on transmitral spectral Doppler velocity-profile analysis, 1125

Hamato, N., Moriyasu, F., Someda, H., Nishikawa, K., Chiba, T. and Okuma, M.: phase shift of the hepatic vein flow velocity waveform in chronic liver disease: experimental and clinical studies, 821

Hamato, N., Moriyasu, F., Someda, H., Nishikawa, K., Chiba, T. and Okuma, M.: clinical application of hepatic venous hemodynamics by Doppler ultrasonography in chronic liver disease, 829

Hansen, F., see Ahlgren, A. R.

Harihara, Y., see Sugawara, Y.

Harmonic imaging
second harmonic characteristics of the ultrasound contrast agents Albunex and FSO69 (Krishna), 453

Harness
Doppler sensors and harnesses for cardiac and peripheral arterial flow monitoring (Arbeille), 415

Harris, M., see Reher, P.

Harvey, W., see Reher, P.

Hatab, M. R., Giller, C. A. and Clarke, G. D.: evaluation of cerebral arterial flow with transcranial Doppler ultrasound: theoretical development and phantom studies, 1025

Head and neck tumors
prognostic significance of color Doppler findings in head and neck tumors (Delorme), 1311

Heart
effects of pulsed ultrasound on the frog heart: III. the radiation force mechanism (Dalecki), 275
thresholds for premature contractions in murine hearts exposed to pulsed ultrasound (MacRobbie), 761

Heating
a numerical study of the effect of drive level on the intensity loss from an ultrasonic beam (Baker), 1083
a thermal beam-shape phantom for ultrasound physiotherapy transducers (Martin), 1267

liver hemostasis using high-intensity focused ultrasound (Vaezy), 1413
temperature rise recorded during lesion formation by high-intensity focused ultrasound (Clarke), 299
the sensitivity of biological tissue to ultrasound (Barnett), 805
ultrasound properties of liver tissue during heating (Gertner), 1395

Heel
quantitative ultrasound of the heel and serum and urinary cortisol values in assessment of long-term corticotherapy side effects in female bronchial asthma patients (Kos-Kudla), 1325

Helton, S., see Vaezy, S.

Helvie, M., see Carson, P. L.

Hemodynamics
an improved flow evaluation scheme in orifices of different aspect ratios (Anayiotos), 231
color flow mapping and hemodynamics (Beach), 319
color flow mapping (Ferrara), 321
differences in the erythrocyte aggregation level between veins and arteries of normolipidemic and hyperlipidemic individuals (Cloutier), 1383

Hemoglobin
minimal static excess pressure minimises the effect of extracorporeal shock waves on cells and reduces it on gallstones (Delius), 611

Hemolysis
acoustic cavitation nuclei survive the apparent ultrasonic destruction of Albunex microspheres (Brayman), 793
correlation of ultrasound-induced hemolysis with cavitation detector output *in vitro* (Everbach), 619
hemolysis *in vivo* from exposure to pulsed ultrasound (Dalecki), 315
hemolysis of 40% hematocrit, Albunex-supplemented human erythrocytes by pulsed ultrasound: frequency, acoustic pressure and pulse length dependence (Brayman), 1237
minimal static excess pressure minimises the effect of extracorporeal shock waves on cells and reduces it on gallstones (Delius), 611
ultrasonically induced hemolysis at high cell and gas body concentrations in a thin-disc exposure chamber (Miller), 625

Hemorrhage
age dependence of ultrasonically induced lung hemorrhage in mice (Dalecki), 767
liver hemostasis using high-intensity focused ultrasound (Vaezy), 1413
remnants of Albunex nucleate acoustic cavitation (Dalecki), 1405
the influence of contrast agents on hemorrhage produced by lithotripter fields (Dalecki), 1435
thresholds for fetal hemorrhages produced by a piezoelectric lithotripter (Dalecki), 287
ultrasonically induced lung hemorrhage in young swine (Dalecki), 777

Henson, B., see Taylor, C. R.

Hepatic artery
intra- and extrahepatic arterial resistances in chronic hepatitis and liver cirrhosis (Piscaglia), 675

Hepatic vein
clinical application of hepatic venous hemodynamics by Doppler ultrasonography in chronic liver disease (Hamato), 829
phase shift of the hepatic vein flow velocity waveform in chronic liver disease: experimental and clinical studies (Hamato), 821

Hepatocellular carcinoma
Doppler ultrasound in the evaluation of cirrhotic patients: the prevalence of intrahepatic arteriovenous shunting, and implications for diagnosis of hepatocellular carcinoma (Taylor), 1155

HIFU
a piezocomposite shock-wave generator with electronic focusing capability: application for producing cavitation-induced lesions in rabbit liver (Tavakkoli), 107
influence of ablated tissue on the formation of high-intensity focused ultrasound lesions (Chen), 921
liver hemostasis using high-intensity focused ultrasound (Vaezy), 1413
minimal static excess pressure minimises the effect of extracorporeal shock waves on cells and reduces it on gallstones (Delius), 611
quantitative acoustic characterization of a new surfactant-based ultrasound contrast agent (Forsberg), 1201
shock-wave measurement using a calibrated interferometric fiber-tip sensor (Koch), 1259
temperature rise recorded during lesion formation by high-intensity focused ultrasound (Clarke), 299
the influence of contrast agents on hemorrhage produced by lithotripter fields (Dalecki), 1435
the sensitivity of biological tissue to ultrasound (Barnett), 805
thresholds for fetal hemorrhages produced by a piezoelectric lithotripter (Dalecki), 287
ultrasound properties of liver tissue during heating (Gertner), 1395

High-frequency imaging
a high-frequency pulsed-wave Doppler ultrasound system for the detection and imaging of blood flow in the microcirculation (Christopher), 997
ultrasonic biomicroscopy of viable, dead and apoptotic cells (Czarnota), 961

Hill, C. R., see Chen, L.

Histology
characterisation of atherosclerotic plaque by spectral analysis of intravascular ultrasound: an *in vitro* methodology (Spencer), 191
correlation of ultrasonic attenuation (30 to 50 MHz) and constituents of atherosclerotic plaque (Bridal), 691
lack of correlation between ultrasonography and histologic staging of the endometrium in *in vitro* fertilization (IVF) patients (Sterzik), 165
parametric (integrated backscatter and attenuation) images constructed using backscattered radiofrequency signals (25–56 MHz) from human aortae *in vitro* (Bridal), 215

History
the history of ultrasound in gynecology 1950–1980 (Levi), 481

Hoeks, A. P. G., see Brands, P. J.

Hoeks, A. P. G., see Samijo, S. K.

Hoeks, A. P. G., Willekes, C., Boutouyrie, P., Brands, P. J., Willigers, J. M. and Reneman, R. S.: automated detection of local artery wall thickness based on M-line signal processing, 1017

Hoffman, J., see Ren, J-F.

Hollerweger, A., Rettenbacher, T., Macheiner, P. and Gritzmann, N.: new signs of breast cancer: high resistance flow and variations in resistive indices evaluation by color Doppler sonography, 851

Hoskins, P. R., see Li, S.

Hoskins, P. R.: peak velocity estimation in arterial stenosis models using colour vector Doppler, 889

Howard, D. and Sturtevant, B.: *in vitro* study of the mechanical effects of shock-wave lithotripsy, 1107

Hsu, K-F., see Chang, F-M.

Hughes, D. I. and Duck, F. A.: automatic attenuation compensation for ultrasonic imaging, 651

Hunt, J. W., see Czarnota, G. J.

Hunt, J. W., see Worthington, A. E.

Husby, P., see Zhou, Y-Q.

Hydrophone
an optical trigger source for hydrophone-based ultrasound measurement systems: a feasibility study (Petley), 755
electromagnetic hydrophone for pressure determination of shock-wave pulses (Etienne), 747
shock-wave measurement using a calibrated interferometric fiber-tip sensor (Koch), 1259

Hyperthermia
ultrasound properties of liver tissue during heating (Gertner), 1395

Hypocalcemia
bone status after long-term anticonvulsant therapy in epileptic patients: evaluation using quantitative ultrasound of calcaneus and phalanges (Pluskiewicz), 553

I

Ikegami, T., see Sugawara, Y.

Image processing
automatic attenuation compensation for ultrasonic imaging (Hughes), 651
characterization of echographic image texture by cooccurrence matrix parameters (Valckx), 559
comparison of B-mode, M-mode and echo-tracking methods for measurement of the arterial distension waveform (Stadler), 879
correlation of ultrasound parameter imaging with microcirculatory patterns in uveal melanomas (Silverman), 573
interactive automatic fetal head measurements from ultrasound images using multimedia computer technology (Pathak), 665
the 3-D and 2-D color flow display of breast masses (Carson), 837

three-dimensional freehand ultrasound: image reconstruction and volume analysis (Barry), 1209
ultrasound contrast agent in intravascular echography: an *in vitro* study (Cachard), 705

Image testing
phantoms and automated system for testing the resolution of ultrasound scanners (Rownd), 245

Image texture
characterization of echographic image texture by cooccurrence matrix parameters (Valckx), 559

Imanaka, M., see Nakai, Y.

Imuta, N., Kinoshita, N., Etani, H., Yagita, Y. and Nukada, T.: the reproducibility of color Doppler duplex sonography in the measurement of renal arterial blood velocity, 813

In vitro *fertilization*
lack of correlation between ultrasonography and histologic staging of the endometrium in *in vitro* fertilization (IVF) patients (Sterzik), 165

In vitro *irradiation*
acoustic cavitation nuclei survive the apparent ultrasonic destruction of Albunex microspheres (Brayman), 793
comparative sensitivity of human erythrocytes and lymphocytes to sonolysis by 1-MHz ultrasound (Miller), 635
correlation of ultrasound-induced hemolysis with cavitation detector output *in vitro* (Everbach), 619
hemolysis of 40% hematocrit, Albunex-supplemented human erythrocytes by pulsed ultrasound: frequency, acoustic pressure and pulse length dependence (Brayman), 1237
in vitro study of the mechanical effects of shock-wave lithotripsy (Howard), 1107
mechanism of ultrasound-enhanced porphyrin cytotoxicity. Part I: a search for free radical effects (Worthington), 1095
minimal static excess pressure minimises the effect of extracorporeal shock waves on cells and reduces it on gallstones (Delius), 611
quantitation of shock-wave cavitation damage *in vitro* (Lifshitz), 461
stress-wave–induced membrane permeation of red blood cells is facilitated by aquaporins (Lee), 1089
the effect of polypropylene vials on lithotripter shock waves (Cleveland), 939
transfection of a reporter plasmid into cultured cells by sonoporation *in vitro* (Bao), 953
ultrasonically induced hemolysis at high cell and gas body concentrations in a thin-disc exposure chamber (Miller), 625
ultrasound properties of liver tissue during heating (Gertner), 1395

In vivo *irradiation*
a piezocomposite shock-wave generator with electronic focusing capability: application for producing cavitation-induced lesions in rabbit liver (Tavakkoli), 107
age dependence of ultrasonically induced lung hemorrhage in mice (Dalecki), 767

effects of pulsed ultrasound on the frog heart: III. the radiation force mechanism (Dalecki), 275
hemolysis *in vivo* from exposure to pulsed ultrasound (Dalecki), 315
influence of ablated tissue on the formation of high-intensity focused ultrasound lesions (Chen), 921
liver hemostasis using high-intensity focused ultrasound (Vaezy), 1413
remnants of Albunex nucleate acoustic cavitation (Dalecki), 1405
thresholds for fetal hemorrhages produced by a piezoelectric lithotripter (Dalecki), 287
thresholds for premature contractions in murine hearts exposed to pulsed ultrasound (MacRobbie), 761
ultrasound stimulation of rat testes damaged by Busulfan (Haddad), 1421

Inoue, K., see Sugawara, Y.

Intensity
a numerical study of the effect of drive level on the intensity loss from an ultrasonic beam (Baker), 1083
a thermal beam-shape phantom for ultrasound physiotherapy transducers (Martin), 1267

Intensity distribution
a numerical study of the effect of drive level on the intensity loss from an ultrasonic beam (Baker), 1083

Interferometry
shock-wave measurement using a calibrated interferometric fiber-tip sensor (Koch), 1259

Interventional ultrasound
characterisation of atherosclerotic plaque by spectral analysis of intravascular ultrasound: an *in vitro* methodology (Spencer), 191

Intimal-medial thickness
variation of common carotid artery elasticity with intimal-medial thickness: the ARIC study (Riley), 157

Intracardiac imaging
lower frequency (5 MHz) intracardiac echocardiography in a large swine model: imaging views and research applications (Ren), 871

Intraoperative ultrasound
intraoperative evaluation of small-calibre arterial reconstructions (Sugawara), 473

Isolated heart cells
effect of ultrasound on the contraction of isolated myocardial cells of adult rats (Salz), 143

IVUS
a study of the quantitative and qualitative impact of catheter shaft angulation in a mechanical intravascular ultrasound system (Kearney), 87
an evaluation of the potential and limitations of three-dimensional reconstructions from intravascular ultrasound images (Thrush), 437
characterisation of atherosclerotic plaque by spectral analysis of intravascular ultrasound: an *in vitro* methodology (Spencer), 191

characterisation of red and white thrombus by intravascular ultrasound using radiofrequency and videodensitometric data-based texture analysis (Ramo), 1195
high-frequency ultrasonic detection of thrombi with a targeted contrast system (Lanza), 863
intravascular elasticity imaging using ultrasound: feasibility studies in phantoms (De Korte), 735
tissue-equivalent vessel phantoms for intravascular ultrasound (Ryan), 261
ultrasound contrast agent in intravascular echography: an *in vitro* study (Cachard), 705

J

Jansson, T., Almqvist, M., Stråhlén, K., Eriksson, R., Sparr, G., Persson, H. W. and Lindström, K.: ultrasound Doppler vector tomography measurements of directional blood flow, 47

Jespersen, S. K., see Wilhjelm, J. E.

Joern, H., Klein, A., Kuehlwein, H. and Rath, W.: critical comparison of indices and threshold values for assessing placenta performance using Doppler ultrasound, 1179

John, N. W., see Barry, C. D.

Johnston, K. W., see Bascom, P. A. J.

Justin, J., see Noritomi, T.

K

Kaczowski, P., see Vaezy, S.

Kaiser, S., see Dost, P.

Kalisz, A., see Lizzi, F. L.

Kallel, F., Varghese, T., Ophir, J. and Bilgen, M.: the nonstationary strain filter in elastography: Part II. lateral and elevational decorrelation, 1357

Kawasaki, S., see Kitamura, H.

Kearney, P. P., Ramo, M. P., Spencer, T., Shaw, R. R. D., Starkey, I. R., McDicken, N. and Sutherland, G. R.: a study of the quantitative and qualitative impact of catheter shaft angulation in a mechanical intravascular ultrasound system, 87

Kearney, P. P., see Ramo, M. P.

Kearney, P. P., see Spencer, T.

Keeton, P. I. J., Schlindwein, F. S. and Evans, D. H.: a study of the spectral broadening of simulated Doppler signals using FFT and AR modelling, 1033

Keilman, G., see Vaezy, S.

Kerscher, M. J., see Göttlober, P.

Keselbrener, L., see Tepper, R.

Kidney
contrast ultrasonography for 2-D opacification of heart cavities, peripheral vessels, kidney and muscle (Strauss), 975

the reproducibility of color Doppler duplex sonography in the measurement of renal arterial blood velocity (Imuta), 813

Kim, Y., see Pathak, S. D.

Kimura, H., see Sugawara, Y.

Kinoshita, N., see Imuta, N.

Kisslo, J., see Ota, T.

Kitamura, H. and Kawasaki, S.: detection and clinical significance of red cell aggregation in the human subcutaneous vein using a high-frequency transducer (10 MHz): a preliminary report, 933

Kitslaar, P. J. E. H. M., see Samijo, S. K.

Klein, A., see Joern, H.

Ko, H-C., see Chang, F-M.

Kobayashi, K., see Kono, Y.

Koch, C., Molkenstruck, W. and Reibold, R.: shock-wave measurement using a calibrated interferometric fiber-tip sensor, 1259

Kojima, M., Watanabe, H., Watanabe, M., Okihara, K., Naya, Y. and Ukimura, O.: preliminary results of power Doppler imaging in benign prostatic hyperplasia, 1305

Kolios, M. C., see Czarnota, G. J.

Koller, M-E., see Zhou, Y-Q.

Kono, Y., Moriyasu, F., Nada, T., Suginoshita, Y., Matsumura, T., Kobayashi, K., Nakamura, T. and Chiba, T.: gray-scale second harmonic imaging of the liver: a preliminary animal study, 719

Korting, H. C., see Göttlober, P.

Kos-Kudla, B. and Pluskiewicz, W.: quantitative ultrasound of the heel and serum and urinary cortisol values in assessment of long-term cortico-therapy side effects in female bronchial asthma patients, 1325

Kovács, S. J., see Hall, A. F.

Krams, R., see van der Steen, A. F. W.

Krishna, P. D. and Newhouse, V. L.: second harmonic characteristics of the ultrasound contrast agents Albunex and FSO69, 453

Kubota, K., see Sugawara, Y.

Kuehlwein, H., see Joern, H.

Kujawska, T., see Etienne, J.

Kutob, S. S., see Thrush, A. J.

L

Laing, T. J., see Chiang, E. H.

Lancée, C. T., see De Korte, C. L.

Lancée, C. T., see van der Steen, A. F. W.

Lange, A., Palka, P., Caso, P., Fenn, L. N., Olszweski, R., Ramo, M. P., Shaw, R. R. D., Nowicki, A., Fox, K. A. A. and Sutherland, G. R.: Doppler myocardial imaging vs. B-mode grey-scale imaging: a comparative *in vitro*

and *in vivo* study into their relative efficacy in endocardial boundary detection, 69

Länne, T., see Ahlgren, A. R.

Lanza, G. M., Wallace, K. D., Fischer, S. E., Christy, D. H., Scott, M. J., Trousil, R. L., Cacheris, W. P., Miller, J. G., Gaffey, P. J. and Wickline, S. A.: high-frequency ultrasonic detection of thrombi with a targeted contrast system, 863

Laser confocal microscopy
ultrasonic characterization of *in vitro* osteoarthritic articular cartilage with validation by confocal microscopy (Chiang), 205

Ledoux, L. A. F., see Brands, P. J.

Lee, S., McAuliffe, D. J., Zhang, H., Xu, Z., Taitelbaum, J., Flotte, T. J. and Doukas, A. G.: stress-wave induced membrane permeation of red blood cells is facilitated by aquaporins, 1089

Lees, R. S., see Stadler, R. W.

Left ventricle
assessment of mitral A-wave transit time to cardiac outflow tract and isovolumic relaxation time of left ventricle in the appropriate and small-for–gestational–age human fetus (Tsyvian), 187
Doppler myocardial imaging vs. B-mode grey-scale imaging: a comparative *in vitro* and *in vivo* study into their relative efficacy in endocardial boundary detection (Lange), 69
echo machine-imposed limit on transmitral spectral Doppler velocity-profile analysis (Hall), 1225

Left ventricular volume
Doppler myocardial imaging vs. B-mode grey-scale imaging: a comparative *in vitro* and *in vivo* study into their relative efficacy in endocardial boundary detection (Lange), 69

Leotta, D. F., Detmer, P. R. and Martin, R. W.: performance of a miniature magnetic position sensor for three-dimensional ultrasound imaging, 597

Lesion formation
a piezocomposite shock-wave generator with electronic focusing capability: application for producing cavitation-induced lesions in rabbit liver (Tavakkoli), 107
influence of ablated tissue on the formation of high-intensity focused ultrasound lesions (Chen), 921
temperature rise recorded during lesion formation by high-intensity focused ultrasound (Clarke), 299

Levi, S.: the history of ultrasound in gynecology 1950–1980, 481

Li, K. S., see Ren, J-F.

Li, R. et al: reproducibility of extracranial carotid atherosclerotic lesions assessed by B-mode ultrasound: the atherosclerosis risk in communities study, 791

Li, S., Hoskins, P. R. and McDicken, W. N.: rapid measurement of the spatial resolution of colour flow scanners, 591

Lifshitz, D. A., Williams, J. C. Jr., Sturtevant, B., Connors, B. A., Evan, A. P. and McAteer, J. A.: quantitation of shock-wave cavitation damage *in vitro*, 461

Lighty Jr., G. W., see Ren, J-F.

Lin, C-J., see Chen, T.

Lindström, K., see Jansson, T.

Lithotripsy
electromagnetic hydrophone for pressure determination of shock-wave pulses (Etienne), 747
in vitro study of the mechanical effects of shock-wave lithotripsy (Howard), 1107
minimal static excess pressure minimises the effect of extracorporeal shock waves on cells and reduces it on gallstones (Delius), 611
quantitation of shock-wave cavitation damage *in vitro* (Lifshitz), 461
remnants of Albunex nucleate acoustic cavitation (Dalecki), 1405
shock-wave measurement using a calibrated interferometric fiber-tip sensor (Koch), 1259
stress-wave induced membrane permeation of red blood cells is facilitated by aquaporins (Lee), 1089
the effect of polypropylene vials on lithotripter shock waves (Cleveland), 939
the influence of contrast agents on hemorrhage produced by lithotripter fields (Dalecki), 1435
thresholds for fetal hemorrhages produced by a piezoelectric lithotripter (Dalecki), 287

Liu, D. D., see Fei, D-Y.

Liver
a piezocomposite shock-wave generator with electronic focusing capability: application for producing cavitation-induced lesions in rabbit liver (Tavakkoli), 107
clinical application of hepatic venous hemodynamics by Doppler ultrasonography in chronic liver disease (Hamato), 829
Doppler ultrasound in the evaluation of cirrhotic patients: the prevalence of intrahepatic arteriovenous shunting, and implications for diagnosis of hepatocellular carcinoma (Taylor), 1155
gray-scale second harmonic imaging of the liver: a preliminary animal study (Kono), 719
influence of ablated tissue on the formation of high-intensity focused ultrasound lesions (Chen), 921
intra- and extrahepatic arterial resistances in chronic hepatitis and liver cirrhosis (Piscaglia), 675
liver hemostasis using high-intensity focused ultrasound (Vaezy), 1413
phase shift of the hepatic vein flow velocity waveform in chronic liver disease: experimental and clinical studies (Hamato), 821
statistical framework for ultrasonic spectral parameter imaging (Lizzi), 1371
temperature rise recorded during lesion formation by high-intensity focused ultrasound (Clarke), 299
three-dimensional ultrasound assessment of fetal liver volume in normal pregnancy: a comparison of reproducibility with two-dimensional ultrasound and a search for a volume constant (Chang), 381
ultrasonic characterization of tissues *via* backscatter frequency dependence (Stetson), 989

ultrasound attenuation and backscatter in the liver during prednisone administration (Lu), 1
ultrasound properties of liver tissue during heating (Gertner), 1395

Liver cirrhosis
clinical application of hepatic venous hemodynamics by Doppler ultrasonography in chronic liver disease (Hamato), 829
Doppler ultrasound in the evaluation of cirrhotic patients: the prevalence of intrahepatic arteriovenous shunting, and implications for diagnosis of hepatocellular carcinoma (Taylor), 1155
intra- and extrahepatic arterial resistances in chronic hepatitis and liver cirrhosis (Piscaglia), 675
phase shift of the hepatic vein flow velocity waveform in chronic liver disease: experimental and clinical studies (Hamato), 821
ultrasonic characterization of tissues *via* backscatter frequency dependence (Stetson), 989

Liver tumor
a piezocomposite shock-wave generator with electronic focusing capability: application for producing cavitation-induced lesions in rabbit liver (Tavakkoli), 107
gray-scale second harmonic imaging of the liver: a preliminary animal study (Kono), 719
influence of ablated tissue on the formation of high-intensity focused ultrasound lesions (Chen), 921

Liver tumor treatment
a piezocomposite shock-wave generator with electronic focusing capability: application for producing cavitation-induced lesions in rabbit liver (Tavakkoli), 107

Liver volume
three-dimensional ultrasound assessment of fetal liver volume in normal pregnancy: a comparison of reproducibility with two-dimensional ultrasound and a search for a volume constant (Chang), 381

Lizzi, F. L., Astor, M., Feleppa, E. J., Shao, M. and Kalisz, A.: statistical framework for ultrasonic spectral parameter imaging, 1371

Lizzi, F. L., see Silverman, R. H.

Lloyd, H. O., see Silverman, R. H.

Longitudinal waves
measurement of velocity and attenuation of shear waves in bovine compact bone using ultrasonic spectroscopy (Wu), 129

Loupas, T., see Fatkin, D.

Lu, Z. F., Zagzebski, J. A., O'Brien, R. T. and Steinberg, H.: ultrasound attenuation and backscatter in the liver during prednisone administration, 1

Luan, H., see Brayman, A. A.

Lumen
comparison of B-mode, M-mode and echo-tracking methods for measurement of the arterial distension waveform (Stadler), 879

ultrasound contrast agent in intravascular echography: an *in vitro* study (Cachard), 705
variation of common carotid artery elasticity with intimal-medial thickness: the ARIC study (Riley), 157

Lung
age dependence of ultrasonically induced lung hemorrhage in mice (Dalecki), 767
thoraxsonography—part I: chest wall and pleura (Mathis), 1131
thoraxsonography—part II: peripheral pulmonary consolidation (Mathis), 1141
ultrasonically induced lung hemorrhage in young swine (Dalecki), 777

Lymph nodes
prognostic significance of color Doppler findings in head and neck tumors (Delorme), 1311

Lymphocyte lysis
comparative sensitivity of human erythrocytes and lymphocytes to sonolysis by 1-MHz ultrasound (Miller), 635

M

Macheiner, P., see Hollerweger, A.

Machine limits
echo machine-imposed limit on transmitral spectral Doppler velocity-profile analysis (Hall), 1225

MacRobbie, A. G., Raeman, C. H., Child, S. Z. and Dalecki, D.: thresholds for premature contractions in murine hearts exposed to pulsed ultrasound, 761

Madsen, E. L., see Rownd, J. J.

Maeda, K., see Barnett, S. B.

Magnetometer
performance of a miniature magnetic position sensor for three-dimensional ultrasound imaging (Leotta), 597

Mahler, F., see Do, D-D.

Makhoul, R. G., see Fei, D-Y.

Makin, I. R. S., see Everbach, E. C.

Makin, I. R. S., see Forsberg, F.

Makuuchi, M., see Sugawara, Y.

Malignant melanoma
correlation of ultrasound parameter imaging with microcirculatory patterns in uveal melanomas (Silverman), 573

Malkin, K., see Tsyvian, P.

Manfredi, C., see Fort, A.

Manor, M., see Tepper, R.

Marinoni, M., Ginanneschi, A., Forleo, P. and Amaducci, L.: technical limits in transcranial Doppler recording: inadequate acoustic windows, 1275

Markus, H. S., see Deane, C. R.

Martin, K. and Fernandez, R.: a thermal beam-shape phantom for ultrasound physiotherapy transducers, 1267

Martin, R. W., see Leotta, D. F.

Martin, R., see Vaezy, S.

Mastik, F., see van der Steen, A. F. W.

Mathis, Gebhard: thoraxsonography—part I: chest wall and pleura, 1131

Mathis, Gebhard: thoraxsonography—part II: peripheral pulmonary consolidation, 1141

Matias, A., see Montenegro, N.

Matre, K., see Zhou, Y-Q.

Matsumura, T., see Kono, Y.

Mayer, R., see Dalecki, D.

McAteer, J. A., see Cleveland, R. O.

McAteer, J. A., see Lifshitz, D. A.

McAuliffe, D. J., see Lee, S.

McDicken, N., see Kearney, P. P.

McDicken, W. N., see Li, S.

McDicken, W. N., see Ramo, M. P.

McDicken, W. N., see Spencer, T.

Mean frequency estimation
a radiofrequency domain complex cross-correlation model to estimate blood flow velocity and tissue motion by means of ultrasound (Brands), 911

Mechanical effects
in vitro study of the mechanical effects of shock-wave lithotripsy (Howard), 1107

Mechanical scanning
a study of the quantitative and qualitative impact of catheter shaft angulation in a mechanical intravascular ultrasound system (Kearney), 87

Mediastinum
thoraxsonography—part II: peripheral pulmonary consolidation (Mathis), 1141

Meghji, S., see Reher, P.

Mehaffey, M. G., see Silverman, R. H.

Mehta, S. and Antich, P.: measurement of shear-wave velocity by ultrasound critical-angle reflectometry (UCR), 1123

Mellor, P. M., see Barry, C. D.

Meltzer, R. S., see Dalecki, D.

Meltzer, R. S., see Everbach, E. C.

Membrane permeability
minimal static excess pressure minimises the effect of extracorporeal shock waves on cells and reduces it on gallstones (Delius), 611
stress-wave–induced membrane permeation of red blood cells is facilitated by aquaporins (Lee), 1089

Mesothelioma
thoraxsonography—part I: chest wall and pleura (Mathis), 1131

Metastases
prognostic significance of color Doppler findings in head and neck tumors (Delorme), 1311

Meyer, C. R., see Chiang, E. H.

MI
hemolysis of 40% hematocrit, Albunex-supplemented human erythrocytes by pulsed ultrasound: frequency, acoustic pressure and pulse length dependence (Brayman), 1237

Mice
remnants of Albunex nucleate acoustic cavitation (Dalecki), 1405
the influence of contrast agents on hemorrhage produced by lithotripter fields (Dalecki), 1435

Michele, J. J., see Ren, J-F.

Microbubbles
correlation of ultrasound-induced hemolysis with cavitation detector output *in vitro* (Everbach), 619
quantitative acoustic characterization of a new surfactant-based ultrasound contrast agent (Forsberg), 1201
ultrasound properties of liver tissue during heating (Gertner), 1395

Microcirculation
a high-frequency pulsed-wave Doppler ultrasound system for the detection and imaging of blood flow in the microcirculation (Christopher), 997
correlation of ultrasound parameter imaging with microcirculatory patterns in uveal melanomas (Silverman), 573

Microscope
a high-frequency pulsed-wave Doppler ultrasound system for the detection and imaging of blood flow in the microcirculation (Christopher), 997
correlation of ultrasonic attenuation (30 to 50 MHz) and constituents of atherosclerotic plaque (Bridal), 691
parametric (integrated backscatter and attenuation) images constructed using backscattered radiofrequency signals (25–56 MHz) from human aortae *in vitro* (Bridal), 215
ultrasonic biomicroscopy of viable, dead and apoptotic cells (Czarnota), 961
ultrasonic characterization of *in vitro* osteoarthritic articular cartilage with validation by confocal microscopy (Chiang), 205
ultrasonic tissue characterization of infarcted myocardium by scanning acoustic microscopy (Saijo), 77
ultrasound in ophthalmology (Fledelius), 365

Microspheres
acoustic cavitation nuclei survive the apparent ultrasonic destruction of Albunex microspheres (Brayman), 793

Middle cerebral artery flow
Doppler sensors and harnesses for cardiac and peripheral arterial flow monitoring (Arbeille), 415
signals from dual-gated TCD systems: curious observations and possible explanations (Smith), 15

Miller, D. L., Gies, R. A. and Chrisler, W. B.: ultrasonically induced hemolysis at high cell and gas body concentrations in a thin-disc exposure chamber, 625

Miller, D. L., see Bao, S.

Miller, J. G., see Lanza, G. M.

Miller, M. W., see Brayman, A. A.

Miller, W. M. and Brayman, A. A.: comparative sensitivity of human erythrocytes and lymphocytes to sonolysis by 1-MHz ultrasound, 635

Minimally invasive thermal therapy
a thermal beam-shape phantom for ultrasound physiotherapy transducers (Martin), 1267
liver hemostasis using high-intensity focused ultrasound (Vaezy), 1413
temperature rise recorded during lesion formation by high-intensity focused ultrasound (Clarke), 299
the sensitivity of biological tissue to ultrasound (Barnett), 805
ultrasound properties of liver tissue during heating (Gertner), 1395

Miyata, T., see Sugawara, Y.

Model
a radiofrequency domain complex cross-correlation model to estimate blood flow velocity and tissue motion by means of ultrasound (Brands), 911
acoustic streaming: comparison of low-amplitude linear model with streaming velocities measured by 32-MHz Doppler (Nowicki), 783
echo machine-imposed limit on transmitral spectral Doppler velocity-profile analysis (Hall), 1225

Molecular delivery
stress-wave–induced membrane permeation of red blood cells is facilitated by aquaporins (Lee), 1089

Molkenstruck, W., see Koch, C.

Molnar, L. J., Caldas, J. G. M. P., Vosta, V. P. and Cerri, G. G.: ophthalmic artery aneurysms: an investigation by duplex scan, 1319

Monitoring
Doppler sensors and harnesses for cardiac and peripheral arterial flow monitoring (Arbeille), 415

Montenegro, N., Matias, A., Areias, J. C. and Barros, H.: ductus venosus revisited: a Doppler blood flow evaluation in the first trimester of pregnancy, 171

Moriyasu, F., see Hamato, N.

Moriyasu, F., see Kono, Y.

Moskalik, A. P., see Carson, P. L.

Mourad, P., see Vaezy, S.

Mouse
age dependence of ultrasonically induced lung hemorrhage in mice (Dalecki), 767
hemolysis *in vivo* from exposure to pulsed ultrasound (Dalecki), 315
thresholds for fetal hemorrhages produced by a piezoelectric lithotripter (Dalecki), 287
thresholds for premature contractions in murine hearts exposed to pulsed ultrasound (MacRobbie), 761

MRI flow mapping
ultrasonic color flow mapping: the visualization of four-dimensional cardiac and vascular flow phenomena using two dimensions and "real time" (Beach), 347

Multimedia
interactive automatic fetal head measurements from ultrasound images using multimedia computer technology (Pathak), 665

Muscle
contrast ultrasonography for 2-D opacification of heart cavities, peripheral vessels, kidney and muscle (Strauss), 975

Myocardial infarction
ultrasonic tissue characterization of infarcted myocardium by scanning acoustic microscopy (Saijo), 77

Myocardial wall thickening
influence of data processing on cyclic variation of integrated backscatter and wall thickness in stunned porcine myocardium (van der Steen), 405

Myocardium
Doppler myocardial imaging vs. B-mode grey-scale imaging: a comparative *in vitro* and *in vivo* study into their relative efficacy in endocardial boundary detection (Lange), 69
effect of ultrasound on the contraction of isolated myocardial cells of adult rats (Salz), 143
influence of data processing on cyclic variation of integrated backscatter and wall thickness in stunned porcine myocardium (van der Steen), 405
influences of ultrasonic machine settings, transducer frequency and placement of region of interest on the measurement of integrated backscatter and cyclic variation (Ota), 1059
ultrasonic tissue characterization of infarcted myocardium by scanning acoustic microscopy (Saijo), 77

N

Nada, T., see Kono, Y.

Nakai, Y., Imanaka, M., Nishio, J. and Ogita, S.: umbilical venous pulsation and regional circulatory disturbance, 1165

Nakamura, T., see Kono, Y.

Namba, T., see Sugawara, Y.

Nanda, N. C., see Anayiotos, A. S.

Narrowband estimation
color flow mapping (Ferrara), 321

Naya, Y., see Kojima, M.

Naylor, A. R., see Smith, J. L.

Neural networks
neural network analysis of Doppler ultrasound blood flow signals: a pilot study (Wright), 683

Newhouse, V. L., see Chabria, Y.

Newhouse, V. L., see Krishna, P. D.

Newman, B. E., see Anayiotos, A. S.

Nishikawa, K., see Hamato, N.

Nishio, J., see Nakai, Y.

Nitta, S-I., see Saijo, Y.

Noise
the nonstationary strain filter in elastography: Part II. lateral and elevational decorrelation (Kallel), 1357

Nonlinear effects
a numerical study of the effect of drive level on the intensity loss from an ultrasonic beam (Baker), 1083
acoustic streaming: comparison of low-amplitude linear model with streaming velocities measured by 32-MHz Doppler (Nowicki), 783

Nonlinear propagation
a numerical study of the effect of drive level on the intensity loss from an ultrasonic beam (Baker), 1083
acoustic streaming: comparison of low-amplitude linear model with streaming velocities measured by 32-MHz Doppler (Nowicki), 783

Noritomi, T., Sigel, B., Swami, V., Justin, J., Gahtan, V., Chen, X., Feleppa, E. J., Roberts, A. B. and Shirouzu, K.: carotid plaque typing by multiparameter ultrasonic tissue characterization, 643

Normolle, D., see Carson, P. L.

Nowakowska, J., see Pluskiewicz, W.

Nowicki, A., Secomski, W. and Wójcik, J.: acoustic streaming: comparison of low-amplitude linear model with streaming velocities measured by 32-MHz Doppler, 783

Nowicki, A., see Lange, A.

Nudelman, S. P., see Hall, A. F.

Nukada, T., see Imuta, N.

Numerical model
a numerical study of the effect of drive level on the intensity loss from an ultrasonic beam (Baker), 1083

an improved flow evaluation scheme in orifices of different aspect ratios (Anayiotos), 231
deconvolution process in measurement of arterial velocity profiles *via* an ultrasonic pulsed Doppler velocimeter for evaluation of the wall shear rate (Flaud), 425

O

Obstetrics
ultrasound contrast media and their use in obstetrics and gynecology (Abramowicz), 1287

O'Brien, R. T., see Lu, Z. F.

Ogita, S., see Nakai, Y.

Ohja, M., see Bascom, P. A. J.

Okawai, H., see Saijo, Y.

Okihara, K., see Kojima, M.

Okuma, M., see Hamato, N.

Olszweski, R., see Lange, A.

Ophir, J., see Alam, S. K.

Ophir, J., see Kallel, F.

Ophir, J., see Varghese, T.

Ophthalmic artery
ophthalmic artery aneurysms: an investigation by duplex scan (Molnar), 1319

Ophthalmology
correlation of ultrasound parameter imaging with microcirculatory patterns in uveal melanomas (Silverman), 573
ophthalmic artery aneurysms: an investigation by duplex scan (Molnar), 1319
recursive autoregressive spectral maps for ocular pathology detection (Fort), 391
ultrasound in ophthalmology (Fledelius), 365

Optical trigger
an optical trigger source for hydrophone-based ultrasound measurement systems: a feasibility study (Petley), 755

Organ movement
ultrasonic measurement of breast tissue motion and the implications for velocity estimation (El-Fallah), 1047

Orientation
performance of a miniature magnetic position sensor for three-dimensional ultrasound imaging (Leotta), 597

Orifice flow field
an improved flow evaluation scheme in orifices of different aspect ratios (Anayiotos), 231

Osteoarthritis
ultrasonic characterization of *in vitro* osteoarthritic articular cartilage with validation by confocal microscopy (Chiang), 205

Osteoporosis
bone status after long-term anticonvulsant therapy in epileptic patients: evaluation using quantitative ultrasound of calcaneus and phalanges (Pluskiewicz), 553
quantitative ultrasound of the heel and serum and urinary cortisol values in assessment of long-term corticotherapy side effects in female bronchial asthma patients (Kos-Kudla), 1325
the assessment of development of bone mass in children by quantitative ultrasound through the proximal phalanxes of the hand (Halaba), 1331

Osteoradionecrosis
the stimulation of bone formation *in vitro* by therapeutic ultrasound (Reher), 1251

Ota, T., Craig, D. M. and Kisslo, J.: influences of ultrasonic machine settings, transducer frequency and placement of region of interest on the measurement of integrated backscatter and cyclic variation, 1059

Ottensmeyer, F. P., see Czarnota, G. J.

Ovarian neoplasm
decay constant of Doppler flow waveform as a possible indicator of ovarian malignancy (Tepper), 1171

Ovary
decay constant of Doppler flow waveform as a possible indicator of ovarian malignancy (Tepper), 1171

P

Palka, P., see Lange, A.

Parametric images
correlation of ultrasonic attenuation (30 to 50 MHz) and constituents of atherosclerotic plaque (Bridal), 691
correlation of ultrasound parameter imaging with microcirculatory patterns in uveal melanomas (Silverman), 573
parametric (integrated backscatter and attenuation) images constructed using backscattered radiofrequency signals (25–56 MHz) from human aortae *in vitro* (Bridal), 215
preliminary study in differential contrast echography (Arditi), 1185
statistical framework for ultrasonic spectral parameter imaging (Lizzi), 1371

Parotid gland
ultrasonographic biometry in salivary glands (Dost), 1299

Pathak, S. D., Chalana, V. and Kim, Y.: interactive automatic fetal head measurements from ultrasound images using multimedia computer technology, 665

Pattern recognition
neural network analysis of Doppler ultrasound blood flow signals: a pilot study (Wright), 683

Paun, M., see Beach, K. W.

Penney, D. P., see Dalecki, D.

Performance
phantoms and automated system for testing the resolution of ultrasound scanners (Rownd), 245

Perfusion
new signs of breast cancer: high resistance flow and variations in resistive indices evaluation by color Doppler sonography (Hollerweger), 851
prognostic significance of color Doppler findings in head and neck tumors (Delorme), 1311
second harmonic characteristics of the ultrasound contrast agents Albunex and FSO69 (Krishna), 453
the 3-D and 2-D color flow display of breast masses (Carson), 837
ultrasound contrast media and their use in obstetrics and gynecology (Abramowicz), 1287

Peripheral limb flow
Doppler sensors and harnesses for cardiac and peripheral arterial flow monitoring (Arbeille), 415

Peripheral vessels
contrast ultrasonography for 2-D opacification of heart cavities, peripheral vessels, kidney and muscle (Strauss), 975

Peronneau, P., see Flaud, P.

Perry, G. J., see Anayiotos, A. S.

Persson, H. W., see Jansson, T.

Petenusci, S. O., see Haddad, S.

Peter, R. U., see Göttlober, P.

Petley, G. W. and Blott, B. H.: an optical trigger source for hydrophone-based ultrasound measurement systems: a feasibility study, 755

Phalanxes
the assessment of development of bone mass in children by quantitative ultrasound through the proximal phalanxes of the hand (Halaba), 1331

Phantom
a thermal beam-shape phantom for ultrasound physiotherapy transducers (Martin), 1267
an evaluation of the potential and limitations of three-dimensional reconstructions from intravascular ultrasound images (Thrush), 437
an experimental study of the reflection from spherical and flat-ended cylindrical targets suitable for fetal Doppler performance assessment (Preston), 117
an improved flow evaluation scheme in orifices of different aspect ratios (Anayiotos), 231
characterisation of atherosclerotic plaque by spectral analysis of intravascular ultrasound: an *in vitro* methodology (Spencer), 191
colour velocity flow measurement: *in vitro* validation and application to human carotid (Deane), 447

direct effects of DC cardioversion on blood echogenicity: an *in vitro* study (Fatkin), 135
evaluation of cerebral arterial flow with transcranial Doppler ultrasound: theoretical development and phantom studies (Hatab), 1025
intravascular elasticity imaging using ultrasound: feasibility studies in phantoms (De Korte), 735
nonGaussian statistical property of the ultrasonic Doppler signal downstream of a severe stenosis (Fontaine), 41
peak velocity estimation in arterial stenosis models using colour vector Doppler (Hoskins), 889
phantoms and automated system for testing the resolution of ultrasound scanners (Rownd), 245
rapid measurement of the spatial resolution of colour flow scanners (Li), 591
reduction of signal decorrelation from mechanical compression of tissues by temporal stretching: applications to elastography (Alam), 95
relation of the flow field distal to a moderate stenosis to the Doppler power (Bascom), 25
three-dimensional freehand ultrasound: image reconstruction and volume analysis (Barry), 1209
tissue-equivalent vessel phantoms for intravascular ultrasound (Ryan), 261
ultrasonic characterization of *in vitro* osteoarthritic articular cartilage with validation by confocal microscopy (Chiang), 205
ultrasonic characterization of tissues *via* backscatter frequency dependence (Stetson), 989
ultrasound Doppler vector tomography measurements of directional blood flow (Jansson), 47

Phase velocity
measurement of velocity and attenuation of shear waves in bovine compact bone using ultrasonic spectroscopy (Wu), 129

Phillips, D. J., see Beach, K. W.

Phonophoresis
stress-wave–induced membrane permeation of red blood cells is facilitated by aquaporins (Lee), 1089

Photoacoustics
stress-wave–induced membrane permeation of red blood cells is facilitated by aquaporins (Lee), 1089

Physiotherapy
a thermal beam-shape phantom for ultrasound physiotherapy transducers (Martin), 1267

Pig
a novel method to measure acoustic speed of bone tissue (Chen), 1337
effects of velocity distribution, diameter measurement and velocity tracing on the accuracy of cardiac output measurement by pulsed Doppler echocardiography in the aortic annulus of pigs (Zhou), 177
influence of data processing on cyclic variation of integrated backscatter and wall thickness in stunned porcine myocardium (van der Steen), 405
lower frequency (5 MHz) intracardiac echocardiography in a large swine model: imaging views and research applications (Ren), 871
ultrasonically induced lung hemorrhage in young swine (Dalecki), 777

Pioneers
the history of ultrasound in gynecology 1950–1980 (Levi), 481

Piscaglia, F., Gaiani, S., Zironi, G., Gramantieri, L., Casali, A., Siringo, S., Serra, C. and Bolondi, L.: Intra- and extrahepatic arterial resistances in chronic hepatitis and liver cirrhosis, 675

Placenta performance
critical comparison of indices and threshold values for assessing placenta performance using Doppler ultrasound (Joern), 1179

Placental imaging
ultrasound contrast media and their use in obstetrics and gynecology (Abramowicz), 1287

Plantec, M. B., see El-Fallah, A. I.

Plaque
carotid plaque typing by multiparameter ultrasonic tissue characterization (Noritomi), 643
characterisation of atherosclerotic plaque by spectral analysis of intravascular ultrasound: an *in vitro* methodology (Spencer), 191
correlation of ultrasonic attenuation (30 to 50 MHz) and constituents of atherosclerotic plaque (Bridal), 691

Plasma macromolecules
detection and clinical significance of red cell aggregation in the human subcutaneous vein using a high-frequency transducer (10 MHz): a preliminary report (Kitamura), 933

Plett, M., see Beach, K. W.

Pleura
thoraxsonography—part I: chest wall and pleura (Mathis), 1131
thoraxsonography—part II: peripheral pulmonary consolidation (Mathis), 1141

Pleura metastases
thoraxsonography—part I: chest wall and pleura (Mathis), 1131

Pleural effusion
thoraxsonography—part I: chest wall and pleura (Mathis), 1131

Pleuritis
thoraxsonography—part I: chest wall and pleura (Mathis), 1131

Pluskiewicz, W. and Nowakowska, J.: bone status after long-term anticonvulsant therapy in epileptic patients: evaluation using quantitative ultrasound of calcaneus and phalanges, 553

Pluskiewicz, W., see Halaba, Z.

Pluskiewicz, W., see Kos-Kudla, B.

Pneumonia
thoraxsonography—part II: peripheral pulmonary consolidation (Mathis), 1141

Pneumothorax
thoraxsonography—part I: chest wall and pleura (Mathis), 1131

Polypropylene
the effect of polypropylene vials on lithotripter shock waves (Cleveland), 939

Popliteal artery
neural network analysis of Doppler ultrasound blood flow signals: a pilot study (Wright), 683
unusual pseudoaneurysms after catheterization: successful treatment by ultrasound-guided compression (Do), 377

Porcine artery
influence of tissue-preservation methods on arterial geometry and echogenicity (Wilhjelm), 1071

Porphyrin cytotoxicity
mechanism of ultrasound-enhanced porphyrin cytotoxicity. Part I: a search for free radical effects (Worthington), 1095

Portal hypertension
intra- and extrahepatic arterial resistances in chronic hepatitis and liver cirrhosis (Piscaglia), 675

Position sensor
performance of a miniature magnetic position sensor for three-dimensional ultrasound imaging (Leotta), 597

Postert, T., Federlein, J., Przuntek, H. and Büttner, T.: insufficient and absent acoustic temporal bone window: potential and limitations of transcranial contrast-enhanced color-coded sonography and contrast-enhanced power-based sonography, 857

Powell, K., see Beach, K. W.

Power Doppler
a high-frequency pulsed-wave Doppler ultrasound system for the detection and imaging of blood flow in the microcirculation (Christopher), 997
color flow mapping (Ferrara), 321
differences in the erythrocyte aggregation level between veins and arteries of normolipidemic and hyperlipidemic individuals (Cloutier), 1383
insufficient and absent acoustic temporal bone window: potential and limitations of transcranial contrast-enhanced color-coded sonography and contrast-enhanced power-based sonography (Postert), 857
preliminary results of power Doppler imaging in benign prostatic hyperplasia (Kojima), 1305

Power spectrum analysis
carotid plaque typing by multiparameter ultrasonic tissue characterization (Noritomi), 643
characterisation of atherosclerotic plaque by spectral analysis of intravascular ultrasound: an *in vitro* methodology (Spencer), 191
recursive autoregressive spectral maps for ocular pathology detection (Fort), 391

Prat, F., see Tavakkoli, J.

Prednisone
ultrasound attenuation and backscatter in the liver during prednisone administration (Lu), 1

Pregnancy complications
critical comparison of indices and threshold values for assessing placenta performance using Doppler ultrasound (Joern), 1179

Premature ventricular contraction
effects of pulsed ultrasound on the frog heart: III. the radiation force mechanism (Dalecki), 275

Pressure dependence
hemolysis of 40% hematocrit, Albunex-supplemented human erythrocytes by pulsed ultrasound: frequency, acoustic pressure and pulse length dependence (Brayman), 1237

Preston, R. C. and Bond, A. D.: an experimental study of the reflection from spherical and flat-ended cylindrical targets suitable for fetal Doppler performance assessment, 117

Primozich, J. F., see Beach, K. W.

Probe
intraoperative evaluation of small-calibre arterial reconstructions (Sugawara), 473

Prognosis
prognostic significance of color Doppler findings in head and neck tumors (Delorme), 1311

Programmed cell death
ultrasonic biomicroscopy of viable, dead and apoptotic cells (Czarnota), 961

Prostate
preliminary results of power Doppler imaging in benign prostatic hyperplasia (Kojima), 1305
statistical framework for ultrasonic spectral parameter imaging (Lizzi), 1371
temperature rise recorded during lesion formation by high-intensity focused ultrasound (Clarke), 299

Protein synthesis
the stimulation of bone formation *in vitro* by therapeutic ultrasound (Reher), 1251

Proximal orifice
an improved flow evaluation scheme in orifices of different aspect ratios (Anayiotos), 231

Proximal phalanges
bone status after long-term anticonvulsant therapy in epileptic patients: evaluation using quantitative ultrasound of calcaneus and phalanges (Pluskiewicz), 553

Przuntek, H., see Postert, T.

Pseudoaneurysm
unusual pseudoaneurysms after catheterization: successful treatment by ultrasound-guided compression (Do), 377

PTA
unusual pseudoaneurysms after catheterization: successful treatment by ultrasound-guided compression (Do), 377

Puberty
the assessment of development of bone mass in children by quantitative ultrasound through the proximal phalanxes of the hand (Halaba), 1331

Pulsatile flow
colour velocity flow measurement: *in vitro* validation and application to human carotid (Deane), 447
relation of the flow field distal to a moderate stenosis to the Doppler power (Bascom), 25
ultrasound Doppler vector tomography measurements of directional blood flow (Jansson), 47

Q

Quality assurance
phantoms and automated system for testing the resolution of ultrasound scanners (Rownd), 245
rapid measurement of the spatial resolution of colour flow scanners (Li), 591
shock-wave measurement using a calibrated interferometric fiber-tip sensor (Koch), 1259
tissue-equivalent vessel phantoms for intravascular ultrasound (Ryan), 261

Quantitative ultrasound
bone status after long-term anticonvulsant therapy in epileptic patients: evaluation using quantitative ultrasound of calcaneus and phalanges (Pluskiewicz), 553
quantitative ultrasound of the heel and serum and urinary cortisol values in assessment of long-term corticotherapy side effects in female bronchial asthma patients (Kos-Kudla), 1325
the assessment of development of bone mass in children by quantitative ultrasound through the proximal phalanxes of the hand (Halaba), 1331
ultrasound attenuation and backscatter in the liver during prednisone administration (Lu), 1

R

Rabbit
a piezocomposite shock-wave generator with electronic focusing capability: application for producing cavitation-induced lesions in rabbit liver (Tavakkoli), 107
gray-scale second harmonic imaging of the liver: a preliminary animal study (Kono), 719
liver hemostasis using high-intensity focused ultrasound (Vaezy), 1413

Radiation fibrosis
sonographic determination of cutaneous and subcutaneous fibrosis after accidental exposure to ionising radiation in the course of the Chernobyl nuclear power plant accident (Gottlöber), 9

Radiation force
effects of pulsed ultrasound on the frog heart: III. the radiation force mechanism (Dalecki), 275

Raeman, C. H., see Brayman, A. A.

Raeman, C. H., see Dalecki, D.

Raeman, C. H., see MacRobbie, A. G.

Rakebrandt, F., see Wright, I. A.

Ramo, M. P., see Kearney, P. P.

Ramo, M. P., see Lange, A.

Ramo, M. P., see Spencer, T.

Ramo, M. P., Spencer, T., Kearney, P. P., Shaw, S. T. R. D., Starkey, I. R., McDicken, W. N. and Fox, K. A. A.: characterisation of red and white thrombus by intravascular ultrasound using radiofrequency and video-densitometric data-based texture analysis, 1195

Rath, W., see Joern, H.

Rats
effect of ultrasound on the contraction of isolated myocardial cells of adult rats (Salz), 143
influence of ablated tissue on the formation of high-intensity focused ultrasound lesions (Chen), 921

Rauth, A. M., see Worthington, A. E.

Red blood cells
comparative sensitivity of human erythrocytes and lymphocytes to sonolysis by 1-MHz ultrasound (Miller), 635
detection and clinical significance of red cell aggregation in the human subcutaneous vein using a high-frequency transducer (10 MHz): a preliminary report (Kitamura), 933
differences in the erythrocyte aggregation level between veins and arteries of normolipidemic and hyperlipidemic individuals (Cloutier), 1383
hemolysis of 40% hematocrit, Albunex-supplemented human erythrocytes by pulsed ultrasound: frequency, acoustic pressure and pulse length dependence (Brayman), 1237
nonGaussian statistical property of the ultrasonic Doppler signal downstream of a severe stenosis (Fontaine), 41
stress-wave–induced membrane permeation of red blood cells is facilitated by aquaporins (Lee), 1089

Red cell aggregation
detection and clinical significance of red cell aggregation in the human subcutaneous vein using a high-frequency transducer (10 MHz): a preliminary report (Kitamura), 933
differences in the erythrocyte aggregation level between veins and arteries of normolipidemic and hyperlipidemic individuals (Cloutier), 1383

Reflection
an experimental study of the reflection from spherical and flat-ended cylindrical targets suitable for fetal Doppler performance assessment (Preston), 117

Refraction
the effect of polypropylene vials on lithotripter shock waves (Cleveland), 939

Registration
performance of a miniature magnetic position sensor for three-dimensional ultrasound imaging (Leotta), 597
three-dimensional freehand ultrasound: image reconstruction and volume analysis (Barry), 1209

Reher, P., Elbeshir, E-N. I., Harvey, W., Meghji, S. and Harris, M.: the stimulation of bone formation *in vitro* by therapeutic ultrasound, 1251

Reibold, R., see Koch, C.

Ren, J-F., Schwartzman, D., Michele, J. J., Li, K. S., Hoffman, J., Brode, S. E., Lighty, G. W. Jr., Dillon, S. M. and Chaudhry, F. A.: lower frequency (5 MHz) intracardiac echocardiography in a large swine model: imaging views and research applications, 871

Renal
the reproducibility of color Doppler duplex sonography in the measurement of renal arterial blood velocity (Imuta), 813

Reneman, R. S., see Brands, P. J.

Reneman, R. S., see Hoeks, A. P. G.

Reneman, R. S., see Samijo, S. K.

Reproducibility
colour velocity flow measurement: *in vitro* validation and application to human carotid (Deane), 447
reproducibility of shear rate and shear stress assessment by means of ultrasound in the common carotid artery of young human males and females (Samijo), 583
the reproducibility of color Doppler duplex sonography in the measurement of renal arterial blood velocity (Imuta), 813
three-dimensional ultrasound assessment of fetal liver volume in normal pregnancy: a comparison of reproducibility with two-dimensional ultrasound and a search for a volume constant (Chang), 381

Resistance index
intra- and extrahepatic arterial resistances in chronic hepatitis and liver cirrhosis (Piscaglia), 675
preliminary results of power Doppler imaging in benign prostatic hyperplasia (Kojima), 1305

Rettenbacher, T., see Hollerweger, A.

RF
automated detection of local artery wall thickness based on M-line signal processing (Hoeks), 1017
characterisation of atherosclerotic plaque by spectral analysis of intravascular ultrasound: an *in vitro* methodology (Spencer), 191
characterisation of red and white thrombus by intravascular ultrasound using radiofrequency and videodensitometric data-based texture analysis (Ramo), 1195
correlation of ultrasonic attenuation (30 to 50 MHz) and constituents of atherosclerotic plaque (Bridal), 691

correlation of ultrasound parameter imaging with microcirculatory patterns in uveal melanomas (Silverman), 573
parametric (integrated backscatter and attenuation) images constructed using backscattered radiofrequency signals (25–56 MHz) from human aortae *in vitro* (Bridal), 215
recursive autoregressive spectral maps for ocular pathology detection (Fort), 391

Rib fracture
thoraxsonography—part I: chest wall and pleura (Mathis), 1131
thoraxsonography—part II: peripheral pulmonary consolidation (Mathis), 1141

Ribcage movement
ultrasonic measurement of breast tissue motion and the implications for velocity estimation (El-Fallah), 1047

Rice, M., see Vaezy, S.

Righi, D., see Tortoli, T.

Rijsterborgh, H., see van der Steen, A. F. W.

Riley, W. A., Evans, G. W., Sharrett, A. R., Burke, G. L. and Barnes, R. W.: variation of common carotid artery elasticity with intimal-medial thickness: the ARIC study, 157

Roberts, A. B., see Noritomi, T.

Rocchi, S., see Fort, A.

Roederer, G. O., see Cloutier, G.

Roelandt, J. R. T. C., see van der Steen, A. F. W.

Rondeau, M. J., see Silverman, R. H.

Rosenbusch, B. E., see Sterzik, K.

Rosenfeld, E. H., see Salz, H.

Rott, H-D., see Barnett, S. B.

Roubidoux, M. A., see Carson, P. L.

Rownd, J. J., Madsen, E. L., Zagzebski, J. A., Frank, G. R. and Dong, F.: phantoms and automated system for testing the resolution of ultrasound scanners, 245

Roy, R., see Vaezy, S.

Rubin, J. M., see Carson, P. L.

Rubin, J. M., see Chiang, E. H.

Rudat, V., see Delorme, S.

Ryan, L. K. and Foster, F. S.: tissue-equivalent vessel phantoms for intravascular ultrasound, 261

S

Safety
age dependence of ultrasonically induced lung hemorrhage in mice (Dalecki), 767
an optical trigger source for hydrophone-based ultrasound measurement systems: a feasibility study (Petley), 755

correlation of ultrasound-induced hemolysis with cavitation detector output *in vitro* (Everbach), 619
hemolysis *in vivo* from exposure to pulsed ultrasound (Dalecki), 315
hemolysis of 40% hematocrit, Albunex-supplemented human erythrocytes by pulsed ultrasound: frequency, acoustic pressure and pulse length dependence (Brayman), 1237
in vitro study of the mechanical effects of shock-wave lithotripsy (Howard), 1107
remnants of Albunex nucleate acoustic cavitation (Dalecki), 1405
temperature rise recorded during lesion formation by high-intensity focused ultrasound (Clarke), 299
the history of ultrasound in gynecology 1950–1980 (Levi), 481
the influence of contrast agents on hemorrhage produced by lithotripter fields (Dalecki), 1435
the sensitivity of biological tissue to ultrasound (Barnett), 805
thresholds for fetal hemorrhages produced by a piezoelectric lithotripter (Dalecki), 287
thresholds for premature contractions in murine hearts exposed to pulsed ultrasound (MacRobbie), 761
transfection of a reporter plasmid into cultured cells by sonoporation *in vitro* (Bao), 953
ultrasonically induced lung hemorrhage in young swine (Dalecki), 777
ultrasound properties of liver tissue during heating (Gertner), 1395

Saijo, Y., Tanaka, M., Okawai, H., Sasaki, H., Nitta, S-I. and Dunn, F.: ultrasonic tissue characterization of infarcted myocardium by scanning acoustic microscopy, new signs of breast cancer: high resistance flow and variations in resistive indices evaluation by color Doppler sonography (Hollerweger), 851

Salivary glands
ultrasonographic biometry in salivary glands (Dost), 1299

Salter, D. M., see Spencer, T.

Salz, H., Rosenfeld, E. H. and Wussling, M.: effect of ultrasound on the contraction of isolated myocardial cells of adult rats, 143

SAM
ultrasonic tissue characterization of infarcted myocardium by scanning acoustic microscopy (Saijo), 77

Samijo, S. K., Willigers, J. M., Brands, P. J., Barkhuysen, R., Reneman, R. S., Kitslaar, P. J. E. H. M. and Hoeks, A. P. G.: reproducibility of shear rate and shear stress assessment by means of ultrasound in the common carotid artery of young human males and females, 583

Sasaki, H., see Saijo, Y.

Sato, O., see Sugawara, Y.

Scattering
automatic attenuation compensation for ultrasonic imaging (Hughes), 651
carotid plaque typing by multiparameter ultrasonic tissue characterization (Noritomi), 643
correlation of ultrasonic attenuation (30 to 50 MHz) and constituents of atherosclerotic plaque (Bridal), 691

correlation of ultrasound parameter imaging with microcirculatory patterns in uveal melanomas (Silverman), 573
detection and clinical significance of red cell aggregation in the human subcutaneous vein using a high-frequency transducer (10 MHz): a preliminary report (Kitamura), 933
differences in the erythrocyte aggregation level between veins and arteries of normolipidemic and hyperlipidemic individuals (Cloutier), 1383
high-frequency ultrasonic detection of thrombi with a targeted contrast system (Lanza), 863
influence of data processing on cyclic variation of integrated backscatter and wall thickness in stunned porcine myocardium (van der Steen), 405
influence of tissue preservation methods on arterial geometry and echogenicity (Wilhjelm), 1071
influences of ultrasonic machine settings, transducer frequency and placement of region of interest on the measurement of integrated backscatter and cyclic variation (Ota), 1059
measurement of shear-wave velocity by ultrasound critical-angle reflectometry (UCR) (Mehta), 1123
nonGaussian statistical property of the ultrasonic Doppler signal downstream of a severe stenosis (Fontaine), 41
parametric (integrated backscatter and attenuation) images constructed using backscattered radiofrequency signals (25–56 MHz) from human aortae *in vitro* (Bridal), 215
preliminary study in differential contrast echography (Arditi), 1185
quantitative acoustic characterization of a new surfactant-based ultrasound contrast agent (Forsberg), 1201
recursive autoregressive spectral maps for ocular pathology detection (Fort), 391
statistical framework for ultrasonic spectral parameter imaging (Lizzi), 1371
ultrasonic biomicroscopy of viable, dead and apoptotic cells (Czarnota), 961
ultrasonic characterization of *in vitro* osteoarthritic articular cartilage with validation by confocal microscopy (Chiang), 205
ultrasonic characterization of tissues *via* backscatter frequency dependence (Stetson), 989
ultrasound attenuation and backscatter in the liver during prednisone administration (Lu), 1
ultrasound properties of liver tissue during heating (Gertner), 1395

Schlindwein, F. S., see Keeton, P. I. J.

Schmiedl, W., see Vaezy, S.

Schneider, M., see Arditi, M.

Schneider, V., see Sterzik, K.

Schwartzman, D., see Ren, J-F.

Scott, M. J., see Lanza, G. M.

Secomski, W., see Nowicki, A.

Second harmonic scattering
second harmonic characteristics of the ultrasound contrast agents Albunex and FSO69 (Krishna), 453

Second harmonic imaging
color flow mapping (Ferrara), 321
gray-scale second harmonic imaging of the liver: a preliminary animal study (Kono), 719

second harmonic characteristics of the ultrasound contrast agents Albunex and FSO69 (Krishna), 453

Segmentation
three-dimensional freehand ultrasound: image reconstruction and volume analysis (Barry), 1209

Serra, C., see Piscaglia, F.

SFGA fetus
assessment of mitral A-wave transit time to cardiac outflow tract and isovolumic relaxation time of left ventricle in the appropriate and small-for–gestational–age human fetus (Tsyvian), 187

Shadowing
automatic attenuation compensation for ultrasonic imaging (Hughes), 651

Shao, M., see Lizzi, F. L.

Sharrett, A. R., see Riley, W. A.

Shaw, R. R. D., see Kearney, P. P.

Shaw, R. R. D., see Lange, A.

Shaw, S. T. R. D., see Ramo, M. P.

Shear rate
an FFT-based flow profiler for high-resolution *in vivo* investigations (Tortoli), 899
reproducibility of shear rate and shear stress assessment by means of ultrasound in the common carotid artery of young human males and females (Samijo), 583

Shear stress
reproducibility of shear rate and shear stress assessment by means of ultrasound in the common carotid artery of young human males and females (Samijo), 583

Shear wave
measurement of shear-wave velocity by ultrasound critical-angle reflectometry (UCR) (Mehta), 1123
measurement of velocity and attenuation of shear waves in bovine compact bone using ultrasonic spectroscopy (Wu), 129

Sherar, M. D., see Czarnota, G. J.

Sherar, M. D., see Gertner, M. R.

Shirouzu, K., see Noritomi, T.

Shock waves
a piezocomposite shock-wave generator with electronic focusing capability: application for producing cavitation-induced lesions in rabbit liver (Tavakkoli), 107
electromagnetic hydrophone for pressure determination of shock-wave pulses (Etienne), 747
in vitro study of the mechanical effects of shock-wave lithotripsy (Howard), 1107
minimal static excess pressure minimises the effect of extracorporeal shock waves on cells and reduces it on gallstones (Delius), 611

quantitation of shock-wave cavitation damage *in vitro* (Lifshitz), 461
remnants of Albunex nucleate acoustic cavitation (Dalecki), 1405
shock-wave measurement using a calibrated interferometric fiber-tip sensor (Koch), 1259
stress-wave induced membrane permeation of red blood cells is facilitated by aquaporins (Lee), 1089
the effect of polypropylene vials on lithotripter shock waves (Cleveland), 939
the influence of contrast agents on hemorrhage produced by lithotripter fields (Dalecki), 1435
thresholds for fetal hemorrhages produced by a piezoelectric lithotripter (Dalecki), 287

Sigel, B., see Noritomi, T.

Signal processing
characterisation of atherosclerotic plaque by spectral analysis of intravascular ultrasound: an *in vitro* methodology (Spencer), 191

Sillesen, H., see Wilhjelm, J. E.

Silverman, R. H., Folberg, R., Boldt, H. C., Lloyd, H. O., Rondeau, M. J., Mehaffey, M. G., Lizzi, F. L. and Coleman, D. J.: correlation of ultrasound parameter imaging with microcirculatory patterns in uveal melanomas, 573

Siringo, S., see Piscaglia, F.

Skin
sonographic determination of cutaneous and subcutaneous fibrosis after accidental exposure to ionising radiation in the course of the Chernobyl nuclear power plant accident (Gottlöber), 9

Skin thickness
sonographic determination of cutaneous and subcutaneous fibrosis after accidental exposure to ionising radiation in the course of the Chernobyl nuclear power plant accident (Gottlöber), 9

Smith, J. L., Evans, D. H. and Naylor, A. R.: analysis of the frequency modulation present in Doppler ultrasound signals may allow differentiation between particulate and gaseous cerebral emboli, 727

Smith, J. L., Evans, D. H. and Naylor, A. R.: signals from dual-gated TCD systems: curious observations and possible explanations, 15

Someda, H., see Hamato, N.

Sommer, G., see Stetson, P.

Sonesson, B., see Ahlgren, A. R.

Sound, see *Speed of sound* and *Velocity of sound*

Sparr, G., see Jansson, T.

Spatial resolution
rapid measurement of the spatial resolution of colour flow scanners (Li), 591

Speckle
characterization of echographic image texture by co-occurrence matrix parameters (Valckx), 559

Spectral analysis
a study of the spectral broadening of simulated Doppler signals using FFT and AR modelling (Keeton), 1033
an FFT-based flow profiler for high-resolution *in vivo* investigations (Tortoli), 899
characterisation of atherosclerotic plaque by spectral analysis of intravascular ultrasound: an *in vitro* methodology (Spencer), 191
preliminary study in differential contrast echography (Arditi), 1185
recursive autoregressive spectral maps for ocular pathology detection (Fort), 391
statistical framework for ultrasonic spectral parameter imaging (Lizzi), 1371

Spectral broadening
a study of the spectral broadening of simulated Doppler signals using FFT and AR modelling (Keeton), 1033

Spectral slope
characterisation of atherosclerotic plaque by spectral analysis of intravascular ultrasound: an *in vitro* methodology (Spencer), 191

Speed of sound
a novel method to measure acoustic speed of bone tissue (Chen), 1337
bone status after long-term anticonvulsant therapy in epileptic patients: evaluation using quantitative ultrasound of calcaneus and phalanges (Pluskiewicz), 553
measurement of shear-wave velocity by ultrasound critical-angle reflectometry (UCR) (Mehta), 1123
measurement of velocity and attenuation of shear waves in bovine compact bone using ultrasonic spectroscopy (Wu), 129
quantitative ultrasound of the heel and serum and urinary cortisol values in assessment of long-term corticotherapy side effects in female bronchial asthma patients (Kos-Kudla), 1325
the assessment of development of bone mass in children by quantitative ultrasound through the proximal phalanxes of the hand (Halaba), 1331
ultrasonic tissue characterization of infarcted myocardium by scanning acoustic microscopy (Saijo), 77

Spencer, T., Ramo, M. P., Salter, D. M., Anderson, T., Kearney, P. P., Sutherland, G. R., Fox, K. A. A. and McDicken, W. N.: characterisation of atherosclerotic plaque by spectral analysis of intravascular ultrasound: an *in vitro* methodology, 191

Spencer, T., see Kearney, P. P.

Spencer, T., see Ramo, M. P.

Sperm production
ultrasound stimulation of rat testes damaged by Busulfan (Hadidad), 1421

Spherical
phantoms and automated system for testing the resolution of ultrasound scanners (Rownd), 245

Spontaneous echo contrast
differences in the erythrocyte aggregation level between veins and arteries of normolipidemic and hyperlipidemic individuals (Cloutier), 1383

direct effects of DC cardioversion on blood echogenicity: an *in vitro* study (Fatkin), 135

Stadler, R. W., Taylor, J. A. and Lees, R. S.: comparison of B-mode, M-mode and echo-tracking methods for measurement of the arterial distension waveform, 879

Standards
an experimental study of the reflection from spherical and flat-ended cylindrical targets suitable for fetal Doppler performance assessment (Preston), 117

Starkey, I. R., see Kearney, P. P.

Starkey, I. R., see Ramo, M. P.

Starkoski, B. G., see Christopher, D. A.

Steady flow
nonGaussian statistical property of the ultrasonic Doppler signal downstream of a severe stenosis (Fontaine), 41

Steinberg, H., see Lu, Z. F.

Stenosis
nonGaussian statistical property of the ultrasonic Doppler signal downstream of a severe stenosis (Fontaine), 41
peak velocity estimation in arterial stenosis models using colour vector Doppler (Hoskins), 889
relation of the flow field distal to a moderate stenosis to the Doppler power (Bascom), 25

Steroid hepatopathy
ultrasound attenuation and backscatter in the liver during prednisone administration (Lu), 1

Steroid therapy
quantitative ultrasound of the heel and serum and urinary cortisol values in assessment of long-term corticotherapy side effects in female bronchial asthma patients (Kos-Kudla), 1325

Sterzik, K., Grab, D., Schneider, V., Strehler, E. J., Gagsteiger, F. and Rosenbusch, B. E.: lack of correlation between ultrasonography and histologic staging of the endometrium in *in vitro* fertilization (IVF) patients, 165

Stetson, P. and Sommer, G.: ultrasonic characterization of tissues *via* backscatter frequency dependence, 989

Stiffness
assessment of mitral A-wave transit time to cardiac outflow tract and isovolumic relaxation time of left ventricle in the appropriate and small-for–gestational–age human fetus (Tsyvian), 187
automated detection of local artery wall thickness based on M-line signal processing (Hoeks), 1017
stiffness and diameter of the common carotid artery and abdominal aorta in women (Ahlgren), 983
variation of common carotid artery elasticity with intimal-medial thickness: the ARIC study (Riley), 157

Stimulation threshold
effect of ultrasound on the contraction of isolated myocardial cells of adult rats (Salz), 143

Stråhlén, K., see Jansson, T.

Strain
intravascular elasticity imaging using ultrasound: feasibility studies in phantoms (De Korte), 735
on the use of envelope and RF signal decorrelation as tissue strain estimators (Alam), 1427
reduction of signal decorrelation from mechanical compression of tissues by temporal stretching: applications to elastography (Alam), 95
the nonstationary strain filter in elastography: Part I. frequency-dependent attenuation (Varghese), 1343
the nonstationary strain filter in elastography: Part II. lateral and elevational decorrelation (Kallel), 1357

Strain filter
the nonstationary strain filter in elastography: Part I. frequency-dependent attenuation (Varghese), 1343
the nonstationary strain filter in elastography: Part II. lateral and elevational decorrelation (Kallel), 1357

Strandness, D. E. Jr., see Beach, K. W.

Strauss, A. L. and Beller, K-D.: contrast ultrasonography for 2-D opacification of heart cavities, peripheral vessels, kidney and muscle, 975

Streaming
a numerical study of the effect of drive level on the intensity loss from an ultrasonic beam (Baker), 1083
acoustic streaming: comparison of low-amplitude linear model with streaming velocities measured by 32-MHz Doppler (Nowicki), 783
effect of ultrasound on the contraction of isolated myocardial cells of adult rats (Salz), 143

Strehler, E. J., see Sterzik, K.

Stress
reduction of signal decorrelation from mechanical compression of tissues by temporal stretching: applications to elastography (Alam), 95

Strickler, P. L., see Brayman, A. A.

Sturtevant, B., see Howard, D.

Sturtevant, B., see Lifshitz, D. A.

Submandibular gland
ultrasonographic biometry in salivary glands (Dost), 1299

Sugawara, Y., Ikegami, T., Namba, T., Kimura, H., Inoue, K., Kubota, K., Harihara, Y., Miyata, T., Sato, O., Takayama, T. and Makuuchi, M.: intraoperative evaluation of small-calibre arterial reconstructions, 473

Suginoshita, Y., see Kono, Y.

Surface roughness
ultrasonic characterization of *in vitro* osteoarthritic articular cartilage with validation by confocal microscopy (Chiang), 205

Surgery
a piezocomposite shock wave generator with electronic focusing capability: application for producing cavitation-induced lesions in rabbit liver (Tavakkoli), 107
influence of ablated tissue on the formation of high-intensity focused ultrasound lesions (Chen), 921
liver hemostasis using high-intensity focused ultrasound (Vaezy), 1413
mechanism of ultrasound-enhanced porphyrin cytotoxicity. Part I: a search for free radical effects (Worthington), 1095
temperature rise recorded during lesion formation by high-intensity focused ultrasound (Clarke), 299
the sensitivity of biological tissue to ultrasound (Barnett), 805

Sutherland, G. R., see Lange, A.

Sutherland, G. R., see Spencer, T.

Sutherland, G. R., see Kearney, P. P.

Swami, V., see Noritomi, T.

Swine
a novel method to measure acoustic speed of bone tissue (Chen), 1337
effects of velocity distribution, diameter measurement and velocity tracing on the accuracy of cardiac output measurement by pulsed Doppler echocardiography in the aortic annulus of pigs (Zhou), 177
influence of data processing on cyclic variation of integrated backscatter and wall thickness in stunned porcine myocardium (van der Steen), 405
lower frequency (5 MHz) intracardiac echocardiography in a large swine model: imaging views and research applications (Ren), 871
ultrasonically induced lung hemorrhage in young swine (Dalecki), 777

T

Tabib, A., see Cachard, C.

Taitelbaum, J., see Lee, S.

Takayama, T., see Sugawara, Y.

Tanaka, M., see Saijo, Y.

Tardif, F., see Cloutier, G.

Tavakkoli, J., Birer, A., Arefiev, A., Prat, F., Chapelon, J-Y. and Cathignol, D.: a piezocomposite shock-wave generator with electronic focusing capability: application for producing cavitation-induced lesions in rabbit liver, 107

Taylor, C. R., Garcia-Tsao, G., Henson, B., Case, C. Q. and Taylor, K. J. W.: Doppler ultrasound in the evaluation of cirrhotic patients: the prevalence of intrahepatic arteriovenous shunting, and implications for diagnosis of hepatocellular carcinoma, 1155

Taylor, J. A., see Stadler, R. W.

Taylor, K. J. W., see Taylor, C. R.

Taylor, S., see Vaezy, S.

TCD
Doppler sensors and harnesses for cardiac and peripheral arterial flow monitoring (Arbeille), 415

evaluation of cerebral arterial flow with transcranial Doppler ultrasound: theoretical development and phantom studies (Hatab), 1025
insufficient and absent acoustic temporal bone window: potential and limitations of transcranial contrast-enhanced color-coded sonography and contrast-enhanced power-based sonography (Postert), 857
signals from dual-gated TCD systems: curious observations and possible explanations (Smith), 15
ultrasonic color flow mapping: the visualization of four-dimensional cardiac and vascular flow phenomena using two dimensions and "real time" (Beach), 347

Temperature
a thermal beam-shape phantom for ultrasound physiotherapy transducers (Martin), 1267
liver hemostasis using high-intensity focused ultrasound (Vaezy), 1413
temperature rise recorded during lesion formation by high-intensity focused ultrasound (Clarke), 299
the sensitivity of biological tissue to ultrasound (Barnett), 805
ultrasound properties of liver tissue during heating (Gertner), 1395

Temporal bone
insufficient and absent acoustic temporal bone window: potential and limitations of transcranial contrast-enhanced color-coded sonography and contrast-enhanced power-based sonography (Postert), 857

Temporal stretching
reduction of signal decorrelation from mechanical compression of tissues by temporal stretching: applications to elastography (Alam), 95

Tepper, R., Keselbrener, L., Manor, M., Eyal, S., Beyth, Y., Zimmer, Y. and Akselrod, S.: decay constant of Doppler flow waveform as a possible indicator of ovarian malignancy, 1171

Texture
characterisation of red and white thrombus by intravascular ultrasound using radiofrequency and videodensitometric data-based texture analysis (Ramo), 1195
characterization of echographic image texture by co-occurrence matrix parameters (Valckx), 559

TGC
influences of ultrasonic machine settings, transducer frequency and placement of region of interest on the measurement of integrated backscatter and cyclic variation (Ota), 1059

Therapy
a piezocomposite shock-wave generator with electronic focusing capability: application for producing cavitation-induced lesions in rabbit liver (Tavakkoli), 107
a thermal beam-shape phantom for ultrasound physiotherapy transducers (Martin), 1267
liver hemostasis using high-intensity focused ultrasound (Vaezy), 1413
minimal static excess pressure minimises the effect of extracorporeal shock waves on cells and reduces it on gallstones (Delius), 611

temperature rise recorded during lesion formation by high-intensity focused ultrasound (Clarke), 299
the stimulation of bone formation *in vitro* by therapeutic ultrasound (Reher), 1251
thresholds for fetal hemorrhages produced by a piezoelectric lithotripter (Dalecki), 287
ultrasound properties of liver tissue during heating (Gertner), 1395
ultrasound stimulation of rat testes damaged by Busulfan (Haddad), 1421

Thermal effects
a thermal beam-shape phantom for ultrasound physiotherapy transducers (Martin), 1267
liver hemostasis using high-intensity focused ultrasound (Vaezy), 1413
temperature rise recorded during lesion formation by high-intensity focused ultrasound (Clarke), 299
the sensitivity of biological tissue to ultrasound (Barnett), 805
ultrasound properties of liver tissue during heating (Gertner), 1395

Thermodilution
effects of velocity distribution, diameter measurement and velocity tracing on the accuracy of cardiac output measurement by pulsed Doppler echocardiography in the aortic annulus of pigs (Zhou), 177

Thijssen, J. M., see Valckx, F. M. J.

Thompson, J., see Worthington, A. E.

Thomson, D. S., see Barry, C. D.

Thoraxsonography
thoraxsonography—part I: chest wall and pleura (Mathis), 1131
thoraxsonography—part II: peripheral pulmonary consolidation (Mathis), 1141

Thrall, B. D., see Bao, S.

Thresholds
age dependence of ultrasonically induced lung hemorrhage in mice (Dalecki), 767
hemolysis *in vivo* from exposure to pulsed ultrasound (Dalecki), 315
thresholds for fetal hemorrhages produced by a piezoelectric lithotripter (Dalecki), 287
thresholds for premature contractions in murine hearts exposed to pulsed ultrasound (MacRobbie), 761
ultrasonically induced lung hemorrhage in young swine (Dalecki), 777

Thrombolembolism
direct effects of DC cardioversion on blood echogenicity: an *in vitro* study (Fatkin), 135

Thrombus
carotid plaque typing by multiparameter ultrasonic tissue characterization (Noritomi), 643
characterisation of red and white thrombus by intravascular ultrasound using radiofrequency and videodensitometric data-based texture analysis (Ramo), 1195

high-frequency ultrasonic detection of thrombi with a targeted contrast system (Lanza), 863

Thrush, A. J., Bonnett, D. E., Eliott, M. R., Kutob, S. S. and Evans, D. H.: an evaluation of the potential and limitations of three-dimensional reconstructions from intravascular ultrasound images, 437

Tibia
a novel method to measure acoustic speed of bone tissue (Chen), 1337

Tissue ablation
influence of ablated tissue on the formation of high-intensity focused ultrasound lesions (Chen), 921

Tissue characterisation
analysis of the frequency modulation present in Doppler ultrasound signals may allow differentiation between particulate and gaseous cerebral emboli (Smith), 727
automatic attenuation compensation for ultrasonic imaging (Hughes), 651
carotid plaque typing by multiparameter ultrasonic tissue characterization (Noritomi), 643
characterisation of atherosclerotic plaque by spectral analysis of intravascular ultrasound: an *in vitro* methodology (Spencer), 191
characterisation of red and white thrombus by intravascular ultrasound using radiofrequency and videodensitometric data-based texture analysis (Ramo), 1195
characterization of echographic image texture by co-occurrence matrix parameters (Valckx), 559
correlation of ultrasonic attenuation (30 to 50 MHz) and constituents of atherosclerotic plaque (Bridal), 691
Doppler myocardial imaging vs. B-mode grey-scale imaging: a comparative *in vitro* and *in vivo* study into their relative efficacy in endocardial boundary detection (Lange), 69
influence of data processing on cyclic variation of integrated backscatter and wall thickness in stunned porcine myocardium (van der Steen), 405
influences of ultrasonic machine settings, transducer frequency and placement of region of interest on the measurement of integrated backscatter and cyclic variation (Ota), 1059
parametric (integrated backscatter and attenuation) images constructed using backscattered radiofrequency signals (25–56 MHz) from human aortae *in vitro* (Bridal), 215
phantoms and automated system for testing the resolution of ultrasound scanners (Rownd), 245
preliminary results of power Doppler imaging in benign prostatic hyperplasia (Kojima), 1305
quantitative acoustic characterization of a new surfactant-based ultrasound contrast agent (Forsberg), 1201
recursive autoregressive spectral maps for ocular pathology detection (Fort), 391
reduction of signal decorrelation from mechanical compression of tissues by temporal stretching: applications to elastography (Alam), 95
sonographic determination of cutaneous and subcutaneous fibrosis after accidental exposure to ionising radiation in the course of the Chernobyl nuclear power plant accident (Gottlöber), 9
statistical framework for ultrasonic spectral parameter imaging (Lizzi), 1371

the history of ultrasound in gynecology 1950–1980 (Levi), 481 (Historical Review)
three-dimensional ultrasound assessment of fetal liver volume in normal pregnancy: a comparison of reproducibility with two-dimensional ultrasound and a search for a volume constant (Chang), 381
tissue equivalent vessel phantoms for intravascular ultrasound (Ryan), 261
ultrasonic characterization of *in vitro* osteoarthritic articular cartilage with validation by confocal microscopy (Chiang), 205
ultrasonic characterization of tissues *via* backscatter frequency dependence (Stetson), 989
ultrasonic tissue characterization of infarcted myocardium by scanning acoustic microscopy (Saijo), 77
ultrasound attenuation and backscatter in the liver during prednisone administration (Lu), 1
ultrasound in ophthalmology (Fledelius), 365
ultrasound properties of liver tissue during heating (Gertner), 1395

Tissue compression
reduction of signal decorrelation from mechanical compression of tissues by temporal stretching: applications to elastography (Alam), 95

Tissue injury
in vitro study of the mechanical effects of shock-wave lithotripsy (Howard), 1107

Tissue-mimicking material
intravascular elasticity imaging using ultrasound: feasibility studies in phantoms (De Korte), 735

Tissue movement
a radiofrequency domain complex cross-correlation model to estimate blood flow velocity and tissue motion by means of ultrasound (Brands), 911
ultrasonic measurement of breast tissue motion and the implications for velocity estimation (El-Fallah), 1047

Tissue perfusion
new signs of breast cancer: high resistance flow and variations in resistive indices evaluation by color Doppler sonography (Hollerweger), 851
prognostic significance of color Doppler findings in head and neck tumors (Delorme), 1311
second harmonic characteristics of the ultrasound contrast agents Albunex and FSO69 (Krishna), 453
the 3-D and 2-D color flow display of breast masses (Carson), 837
ultrasound contrast media and their use in obstetrics and gynecology (Abramowicz), 1287

Tissue preservation
influence of tissue-preservation methods on arterial geometry and echogenicity (Wilhjelm), 1071

Tissue sensitivity
the sensitivity of biological tissue to ultrasound (Barnett), 805

Tissue velocity
ultrasonic measurement of breast tissue motion and the implications for velocity estimation (El-Fallah), 1047

Tortoli, T., Guidi, G., Berti, P., Guidi, F. and Righi, D.: an FFT-based flow profiler for high-resolution *in vivo* investigations, 899

Transducer
intraoperative evaluation of small-calibre arterial reconstructions (Sugawara), 473

Transducer frequency
influences of ultrasonic machine settings, transducer frequency and placement of region of interest on the measurement of integrated backscatter and cyclic variation (Ota), 1059

Transit time broadening
estimation of axial blood velocity using the Doppler equation corrected for broadening (Chabria), 967

Transoesophageal echocardiography
direct effects of DC cardioversion on blood echogenicity: an *in vitro* study (Fatkin), 135
lower frequency (5 MHz) intracardiac echocardiography in a large swine model: imaging views and research applications (Ren), 871
thoraxsonography—part II: peripheral pulmonary consolidation (Mathis), 1141

Transorbital Doppler
ophthalmic artery aneurysms: an investigation by duplex scan (Molnar), 1319

Transvaginal Doppler
ductus venosus revisited: a Doppler blood flow evaluation in the first trimester of pregnancy (Montenegro), 171

Trauma
liver hemostasis using high-intensity focused ultrasound (Vaezy), 1413

Trousil, R. L., see Lanza, G. M.

TRUS
preliminary results of power Doppler imaging in benign prostatic hyperplasia (Kojima), 1305

Tsyvian, P., Malkin, K. and Wladimiroff, J. W.: assessment of mitral A-wave transit time to cardiac outflow tract and isovolumic relaxation time of left ventricle in the appropriate and small-for–gestational–age human fetus, 187

Tumor
a piezocomposite shock-wave generator with electronic focusing capability: application for producing cavitation-induced lesions in rabbit liver (Tavakkoli), 107
decay constant of Doppler flow waveform as a possible indicator of ovarian malignancy (Tepper), 1171

gray-scale second harmonic imaging of the liver: a preliminary animal study (Kono), 719
influence of ablated tissue on the formation of high-intensity focused ultrasound lesions (Chen), 921
new signs of breast cancer: high resistance flow and variations in resistive indices evaluation by color Doppler sonography (Hollerweger), 851
prognostic significance of color Doppler findings in head and neck tumors (Delorme), 1311
the 3-D and 2-D color flow display of breast masses (Carson), 837
ultrasound contrast media and their use in obstetrics and gynecology (Abramowicz), 1287
ultrasound properties of liver tissue during heating (Gertner), 1395

Tumor control
influence of ablated tissue on the formation of high-intensity focused ultrasound lesions (Chen), 921

Tumor flow
decay constant of Doppler flow waveform as a possible indicator of ovarian malignancy (Tepper), 1171
new signs of breast cancer: high resistance flow and variations in resistive indices evaluation by color Doppler sonography (Hollerweger), 851
prognostic significance of color Doppler findings in head and neck tumors (Delorme), 1311
the 3-D and 2-D color flow display of breast masses (Carson), 837
ultrasound contrast media and their use in obstetrics and gynecology (Abramowicz), 1287

Turbulence
nonGaussian statistical property of the ultrasonic Doppler signal downstream of a severe stenosis (Fontaine), 41
relation of the flow field distal to a moderate stenosis to the Doppler power (Bascom), 25

Tzeng, J-S., see Chen, T.

U

Ukimura, O., see Kojima, M.

Ultrasonic biomicroscopy
ultrasonic biomicroscopy of viable, dead and apoptotic cells (Czarnota), 961

Ultrasonic spectroscopy
measurement of velocity and attenuation of shear waves in bovine compact bone using ultrasonic spectroscopy (Wu), 129

Ultrasound critical angle reflectometry (UCR)
measurement of shear-wave velocity by ultrasound critical-angle reflectometry (UCR) (Mehta), 1123

Ultrasound guidance
lack of correlation between ultrasonography and histologic staging of the endometrium in *in vitro* fertilization (IVF) patients (Sterzik), 165
thoraxsonography—part II: peripheral pulmonary consolidation (Mathis), 1141

unusual pseudoaneurysms after catheterization: successful treatment by ultrasound-guided compression (Do), 377

Ultrasound-guided compression repair
unusual pseudoaneurysms after catheterization: successful treatment by ultrasound-guided compression (Do), 377

Umbilical vein
umbilical venous pulsation and regional circulatory disturbance (Nakai), 1165

Uveal lesions
recursive autoregressive spectral maps for ocular pathology detection (Fort), 391

V

Vaezy, S., Martin, R., Schmiedl, W., Caps, M., Taylor, S., Beach, K., Carter, S., Kaczowski, P., Keilman, G., Helton, S., Chandler, W., Mourad, P., Rice, M., Roy, R. and Crum, L.: liver hemostasis using high-intensity focused ultrasound, 1413

Valckx, F. M. J. and Thijssen, J. M.: characterization of echographic image texture by co-occurrence matrix parameters, 559

Valvular regurgitation
an improved flow evaluation scheme in orifices of different aspect ratios (Anayiotos), 231

van der Steen, A. F. W., Rijsterborgh, H., Lancée, C. T., Mastik, F., Krams, R., Verdouw, P. D., Roelandt, J. R. T. C. and Bom, N.: influence of data processing on cyclic variation of integrated backscatter and wall thickness in stunned porcine myocardium, 405

van der Steen, A. F. W., see de Korte, C. L.

van Kaick, G., see Delorme, S.

Varghese, T. and Ophir, J.: the nonstationary strain filter in elastography: Part I. frequency-dependent attenuation, 1343

Varghese, T., see Kallel, F.

Vascular tissue
correlation of ultrasonic attenuation (30 to 50 MHz) and constituents of atherosclerotic plaque (Bridal), 691
parametric (integrated backscatter and attenuation) images constructed using backscattered radiofrequency signals (25–56 MHz) from human aortae *in vitro* (Bridal), 215

Vaziri, H., see Czarnota, G. J.

Vector fields
ultrasound Doppler vector tomography measurements of directional blood flow (Jansson), 47

Vector tomography
ultrasound Doppler vector tomography measurements of directional blood flow (Jansson), 47

Vein
contrast ultrasonography for 2-D opacification of heart cavities, peripheral vessels, kidney and muscle (Strauss), 975
detection and clinical significance of red cell aggregation in the human subcutaneous vein using a high-frequency transducer (10 MHz): a preliminary report (Kitamura), 933
differences in the erythrocyte aggregation level between veins and arteries of normolipidemic and hyperlipidemic individuals (Cloutier), 1383

Velocity distribution
effects of velocity distribution, diameter measurement and velocity tracing on the accuracy of cardiac output measurement by pulsed Doppler echocardiography in the aortic annulus of pigs (Zhou), 177

Velocity estimation
ultrasonic measurement of breast tissue motion and the implications for velocity estimation (El-Fallah), 1047

Velocity of sound
a novel method to measure acoustic speed of bone tissue (Chen), 1337
bone status after long-term anticonvulsant therapy in epileptic patients: evaluation using quantitative ultrasound of calcaneus and phalanges (Pluskiewicz), 553
measurement of shear-wave velocity by ultrasound critical-angle reflectometry (UCR) (Mehta), 1123
measurement of velocity and attenuation of shear waves in bovine compact bone using ultrasonic spectroscopy (Wu), 129
quantitative ultrasound of the heel and serum and urinary cortisol values in assessment of long-term corticotherapy side effects in female bronchial asthma patients (Kos-Kudla), 1325
the assessment of development of bone mass in children by quantitative ultrasound through the proximal phalanxes of the hand (Halaba), 1331
ultrasonic tissue characterization of infarcted myocardium by scanning acoustic microscopy (Saijo), 77

Velocity profile
an improved flow evaluation scheme in orifices of different aspect ratios (Anayiotos), 231
deconvolution process in measurement of arterial velocity profiles *via* an ultrasonic pulsed Doppler velocimeter for evaluation of the wall shear rate (Flaud), 425
echo machine-imposed limit on transmitral spectral Doppler velocity-profile analysis (Hall), 1225
effects of velocity distribution, diameter measurement and velocity tracing on the accuracy of cardiac output measurement by pulsed Doppler echocardiography in the aortic annulus of pigs (Zhou), 177

Velocity waveform
clinical application of hepatic venous hemodynamics by Doppler ultrasonography in chronic liver disease (Hamato), 829
phase shift of the hepatic vein flow velocity waveform in chronic liver disease: experimental and clinical studies (Hamato), 821

Venous pulsation
umbilical venous pulsation and regional circulatory disturbance (Nakai), 1165

Verdouw, P. D., see van der Steen, A. F. W.

Vessel diameter
influence of tissue-preservation methods on arterial geometry and echogenicity (Wilhjelm), 1071

Veterinary ultrasound
ultrasound attenuation and backscatter in the liver during prednisone administration (Lu), 1

Videodensitometry
detection and clinical significance of red cell aggregation in the human subcutaneous vein using a high-frequency transducer (10 MHz): a preliminary report (Kitamura), 933

Vogt, K., see Wilhjelm, J. E.

Volume measurement
three-dimensional freehand ultrasound: image reconstruction and volume analysis (Barry), 1209
three-dimensional ultrasound assessment of fetal liver volume in normal pregnancy: a comparison of reproducibility with two-dimensional ultrasound and a search for a volume constant (Chang), 381

Vorticity
ultrasound Doppler vector tomography measurements of directional blood flow (Jansson), 47

Vosta, V. P., see Molnar, L. J.

W

Wahab, M., see Wright, I. A.

Walker, D.: transvaginal ultrasound in infertility, 969

Wall filters
color flow mapping (Ferrara), 321

Wall shear rate
deconvolution process in measurement of arterial velocity profiles *via* an ultrasonic pulsed Doppler velocimeter for evaluation of the wall shear rate (Flaud), 425
reproducibility of shear rate and shear stress assessment by means of ultrasound in the common carotid artery of young human males and females (Samijo), 583

Wall shear stress
reproducibility of shear rate and shear stress assessment by means of ultrasound in the common carotid artery of young human males and females (Samijo), 583

Wall thickening
influence of data processing on cyclic variation of integrated backscatter and wall thickness in stunned porcine myocardium (van der Steen), 405

Wall thickness
automated detection of local artery wall thickness based on M-line signal processing (Hoeks), 1017
influence of data processing on cyclic variation of integrated backscatter and wall thickness in stunned porcine myocardium (van der Steen), 405
influence of tissue-preservation methods on arterial geometry and echogenicity (Wilhjelm), 1071

Wallace, K. D., see Lanza, G. M.

Wang, W., see Forsberg, F.

Watanabe, H., see Kojima, M.

Watanabe, M., see Kojima, M.

Waterton, J. C., see Barry, C. D.

Weng, X., see Cloutier, G.

Wheatley, M. A., see Forsberg, F.

Wickline, S. A., see Lanza, G. M.

Wide band estimation
color flow mapping (Ferrara), 321

Wilhjelm, J. E., Vogt, K., Jespersen, S. K. and Sillesen, H.: influence of tissue-preservation methods on arterial geometry and echogenicity, 1071

Willekes, C., see Hoeks, A. P. G.

Williams, J. C. Jr., see Lifshitz, D. A.

Willigers, J. M., see Hoeks, A. P. G.

Willigers, J. M., see Samijo, S. K.

Wilson, B. C., see Gertner, M. R.

Wladimiroff, J. W., see Tsyvian, P.

Wójcik, J., see Nowicki, A.

Woodchuck
gray-scale second harmonic imaging of the liver: a preliminary animal study (Kono), 719

Woodcock, J. P., see Wright, I. A.

Worthington, A. E., Thompson, J., Rauth, A. M. and Hunt, J. W.: mechanism of ultrasound-enhanced porphyrin cytotoxicity. Part I: a search for free radical effects, 1095

Wound healing
the stimulation of bone formation *in vitro* by therapeutic ultrasound (Reher), 1251

Wright, I. A., Gough, N. A. J., Rakebrandt, F., Wahab, M. and Woodcock, J. P.: neural network analysis of Doppler ultrasound blood flow signals: a pilot study, 683

Wu, J. and Cubberley, F.: measurement of velocity and attenuation of shear waves in bovine compact bone using ultrasonic spectroscopy, 129

Wu, Y., see Forsberg, F.

Wussling, M., see Salz, H.

X

Xu, Z., see Lee, S.

Y

Yagita, Y., see Imuta, N.

Yao, B-L., see Chang, F-M.

Yu, C-H., see Chang, F-M.

Yuan, C., see Beach, K. W.

Z

Zagzebski, J. A., see Lu, Z. F.

Zagzebski, J. A., see Rownd, J. J.

Zhang, H., see Lee, S.

Zhou, Y-Q., Faerestrand, S., Birkeland, S., Matre, K., Husby, P. and Koller, M-E.: effects of velocity distribution, diameter measurement and velocity tracing on the accuracy of cardiac output measurement by pulsed Doppler echocardiography in the aortic annulus of pigs, 177

Zienkiewicz, B., see Etienne, J.

Zimmer, Y., see Tepper, R.

Zironi, G., see Piscaglia, F.

Ziskin, M. C., see Barnett, S. B.

Zuna, I., see Delorme, S.

Journal of Ultrasound in Medicine

The Official Publication of the American Institute of Ultrasound in Medicine

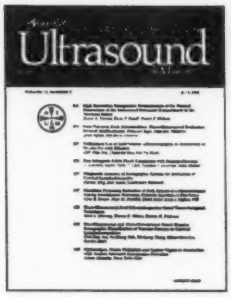

EARN CME CREDITS!!

Earn AMA PRA Category 1 CME credits by reading the *Journal of Ultrasound in Medicine* and returning the monthly CME test.

Don't miss another issue—Subscribe today!

EACH MONTH

Find peer-reviewed papers containing original articles on basic and clinical aspects in ultrasound and advances in the field, techniques, and equipment modifications.

ADDITIONAL FEATURES

- Book Reviews
- Continuing Education
- Bioeffects Literature Reviews
- Product News
- Selected References
- CME Test Credits
- Letters to the Editor

ABOUT THE EDITOR...

George R. Leopold, MD

Dr. Leopold is professor and chair of the Department of Radiology at the University of California, San Diego (UCSD). He received his MD from the University of Pittsburgh School of Medicine in 1962 and has held many positions in the division of ultrasound and radiology departments at UCSD. Dr. Leopold, the editor-in-chief of the *Journal of Ultrasound in Medicine*, also provides editorial guidance to such journals as the *Radiology Resident*, *Clinical Imaging*, and *Clinics in Diagnostic Ultrasound*. He sits on committees in many ultrasound organizations and has won numerous awards from the AIUM during his service, including the 1998 Joseph H. Holmes Clinical Pioneer Award for his outstanding contribution to the growth and development of diagnostic ultrasound.

ORDER FORM

☑YES! I would like to subscribe to the Journal of Ultrasound in Medicine:

Subscription Option (Choose one)

Personal Fee		*Student/Intern-Resident*	
☐ US, Canada, Mexico	$120	☐ US, Canada, Mexico	$72
☐ Outside the US	$155	☐ Outside the US	$93
Agency/Institution Fee		*Additional Fee for Air Mail*	
☐ US, Canada, Mexico	$165	☐ US, Canada, Mexico	$35
☐ Outside the US	$200	☐ Outside the US	$110

** The above prices are effective until October 31, 1998.*

PAYMENT TYPE: (Prepayment required)

___ Check enclosed payable to the AIUM. (U.S. Dollars)

___ Charge my: ☐ VISA ☐ MasterCard ☐ American Express

Card # _____

Expiration Date _____

Signature _____

Your subscription will include all issues from January through December 1998.

SUBSCRIPTION INFORMATION: (Print Clearly)

Name _____

Member # _____

Address _____

_____

_____

Phone _____

Fax _____

E-Mail _____

Orders are not deliverable to post office boxes.

MAIL OR FAX THIS FORM TO:

AIUM
Attn: Subscription Dept.
14750 Sweitzer Lane, Suite 100
Laurel, MD 20707-5906, USA
Fax: 301–498–4450
Phone: 800–638–5352 • 301–498–4100
Website: www.aium.org

Source Code: UMB78

Well illustrated overview of the methods in the assessment of physiological and pathophysiological changes in cerebral hemodynamics and neurosonology

New Trends in Cerebral Hemodynamics and Neurosonology

Edited by **J. Klingelhöfer, E. Bartels** and **E.B. Ringelstein**

This book's intention with its many illustrations and tables is to give the reader an overview of the efficancy of the methods used in the assessment of physiological and pathophysiological changes in cerebral hemodynamics and neurosonology.
Besides the selected contributions of the Symposium on Cerebral Hemodynamics, this book includes additional overview articles on methodological aspects of selected investigation procedures, such as cerebral emboli detection.

***Abbreviated Contents*: Preface. I.Carotid and Vertebrobasilar Occlusive Disease.** Overview of ultrasound in cerebrovascular disease patients (L.R. Caplan). Quantification of carotid stenosis: a fiction? (E.B. Ringelstein). Plaque volume measurements of carotid artery using a magnetic sensor system (A. Delcker). Ultrasound densitometric analysis of carotid plaque composition: patho-anatomic correlation® (Y. Beletsky *et al.*). **II. Clinical Impact of Ultrasonography and Imaging Techniques.** Functional MRI and PET activation studies on the human cortical motor system (H. Boecker). PET and migraine (C. Weiller). Cerebral blood flow (CBF) in chronic hydrocephalus: new aspects (P. Klinge-Xhemajli *et al.*). Regional cerebral perfusion and its reserve compared to CT findings in 100 patients with cerebrovascular disease (M. Schreckenberger *et al.*). **III. Transcranial Color-Coded Duplex Ultrasonography.** Transcranial color-coded sonography in cerebral parenchymal disorders (U. Bogdahn *et al.*). Transcranial color-coded duplex sonography in cerebrovascular disease (G. Seidel, M. Kaps). Alteration of the basal limbic system in primary and secondary depression (T. Becker, G. Becker). What advantages has power Doppler imaging in comparison with frequency-based transcranial color-coded duplex ultrasonography in the evaluation of cerebral aneurysms?(E. Bartels *et al.*). **IV. Detection of Cerebral Emboli.** Methodological aspects of microembolic signal detection (H. Markus). Discrimination and characterization of emboli: old and new aspects (W.H. Mess, B.M. Titulaer, R.G.A. Ackerstaff). Microembolic signals and hemorheology. A pilot study (D.G. Nabavi *et al.*). Dynamic of microembolic signals in acute stroke patients: a prospective TCD study (U. Sliwka *et al.*). **VI. Evoked Flow and Functional Testing.** Bilateral transcranial Doppler monitoring during intracarotid amobarbital test (Wada test) (M. Jauss, C. Hornig, W. Dorndorf). TCD study of hemispheric dominance (P. Vitali *et al.*). Evoked flow changes and language lateralisation during reading tests (P. Tiecks, R.L. Haberl, D.W. Newell). The response requirements of nonlanguage problems modulate cerebral hemodynamics (A.E. Varnadore, A.E. Roberts, W.M. McKinney). **VII. Cerebral Autoregulation Testing.** Multimodal monitoring and autoregulation testing in neurosurgical patients (D.W. Newell *et al.*). Autoregulation monitoring by analysis of spontaneous TCD and blood pressure waves (R.R. Diehl *et al.*). Evaluation of a transient hyperaemic response test as a reliable method for testing autoregulation — comparison against the cuff test (P. Smielewski *et al.*). **VIII. Cerebral Monitoring.** The effects of a stroke unit and the clinical significance of acute blood pressure, diabetes, blood sugar, body temperature and spontaneous reperfusion on stroke outcome (H.S. Jörgensen *et al.*). Noninvasive simulation of intracranial pressure curves using transcranial Doppler sonography and blood pressure curves (B. Schmidt *et al.*). Detection of central and peripheral B- and M-waves with transcrania l and laser Doppler-sonography (P. Zunker *et al.*).
Color section. List of contributors. Subject index.

Please quote the code: FGP on all communications

©1997 864 pages Hardbound
Price: NLG 500.00 / US$ 287.50
ISBN 0-444-82631-9

New York
Elsevier Science
Tel: (+1) 212-633-3730
Toll Free number for North American customers:
1-888-4ES-INFO (437-4636)
Fax: (+1) 212-633-3680
E-mail: usinfo-f@elsevier.com

Amsterdam
Elsevier Science
Tel: (+31) 20-485-3757
Fax: (+31) 20-4853432
E-mail: nlinfo-f@elsevier.nl

Tokyo
Elsevier Science
Tel: (+81) 3-5561-5033
Fax: (+81) 3-5561-5047
E-mail: info@elsevier.co.jp

Singapore
Elsevier Science
Tel: (+65) 434-3727
Fax: (+65) 337-2230
E-mail: asiainfo@elsevier.com.sg

The currencies stated with this information are definitive. Dutch Guilder (NLG) prices apply to customers within Europe and Japan only. US Dollar (US$) prices apply to all customers residing outside Europe and Japan. Prices are subject to change without prior notice. If you are a resident of the EuropeanUnion you should either state your Value Added Tax (VAT) number or add the relevant VAT percentage applicable in your country to the total amount.

ELSEVIER

An Imprint of Elsevier Science

7CM01B01

Keeping you abreast of the latest developments in the growing field of sonochemistry

Ultrasonics Sonochemistry

Asian Editor:

T. Ando, *Shiga University of Medical Science, Shiga, Japan*

European Editor:

T. Mason, *Coventry University, Coventry, UK*

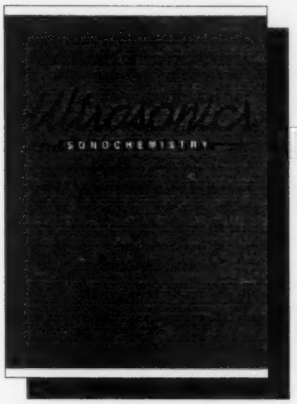

Ultrasonics Sonochemistry has developed out the well-established journal *Ultrasonics* and is available either as a part of the subscription to the main journal or separately on its own. The number of submissions in the area of sonochemistry is increasing since the launch of the journal, necessitating the expansion of the publishing program to four issues in 1997, bringing more research to you more promptly.
Full research papers, short notes, and letters-to-the-Editor are invited in the following areas:

- power ultrasound
- cavitation
- sonoelectrochemistry
- sonoluminescence
- mechanochemistry
- theory and fundamentals
- synthesis: organic, organometallic, inorganic
- biochemical/biomedical aspects
- physical chemical aspects
- industrial applications
- scale-up techniques
- environmental protection
- catalysis, metallurgy

Ultrasonics Sonochemistry is indexed/abstracted in:
Current Contents: Physical, Chemical and Earth Sciences, EI Compendex Plus.

ContentsDirect Now Available.
Elsevier's FREE ContentsDirect service is now available for this journal.
This alerting service sends the table of contents of each issue to your PC 2-4 weeks prior to publication.
To register as a new user, visit the ContentsDirect Web site at http://www.elsevier.com/locate/contentsdirect

Subscription Information:
1998 Volume 5 (in 4 issues)
ISSN 1350-4177
Subscription price: NLG 495.00/US$284.00

Visit our web site for more details about the journal:
http://www.elsevier.nl/locate/ultsonch

For more information or to place an order, contact

For customers in the Americas and Canada
Elsevier Science
P.O. Box 945, New York
N.Y. 10159-0945, U.S.A.
Tel: (+1) 212 633 3730
[Toll Free number for
North-American customers:
1-888-4ES-INFO (437 4636)]
Fax: (+1) 212 633 3680
E-mail: usinfo-f@elsevier.com

For customers in all other locations
Elsevier Science
P.O. Box 211
1000 AE Amsterdam
The Netherlands
Tel: +31(20) 485 3757
Fax: +31(20) 485 3432
E-mail: nlinfo-f@elsevier.nl

FIRST JOINT CONFERENCE OF

ULTRASONICS INTERNATIONAL '99
and
1999 WORLD CONGRESS ON ULTRASONICS

This International Conference and Exhibition will be held 29 June through 1 July 1999 at the Technical University of Denmark, Copenhagen, Denmark.

Technical Co-Chairs:
L. Bjørnø, Techn. Univ. Denmark; **W. Sachse,** Cornell Univ., USA

NDT&E and Bio-medical Ultrasound Tutorials, 28 June 1999.
Chair: D.E. Chimenti, Iowa State Univ., USA.

Ultrasonics International '99 is the 18th Conference in the series which began 35 years ago and the 1999 World Congress on Ultrasonics is the 3rd Conference in the series which began in 1995. At this Joint Conference Special Sessions will be organized by leading international experts on current critical topics of ultrasonics. The programme for the Joint Conference will include invited plenary lectures, contributed oral and poster presentations and an exhibition of most recent industrial and medical ultrasonic products.

Special Sessions:
Applications of AE in manufacturing
Transducers (non-contact)
Medical imaging
Diagnostic ultrasound contrast agents
Inverse problems in ultrasonics
Sonoluminescence
Ultrasonic motors and actuators
High-power ultrasonics in environment and industry
Ultrasonics in the food industry
Ultrasonic enhanced, site-specific, drug delivery
Ultrasonic process monitoring
Blood flow imaging
Non-linear ultrasonic effects
Ultrasonics in complex microstructures
Ultrasonic force and related microscopies
Pico-second acoustics of thin films

Plus Regular Sessions on
all aspects of Ultrasonics

Call for Papers:
Authors are encouraged to submit abstracts for inclusion in the oral and poster sessions by **30th November 1998.** It is important that sufficient information is included in the abstract to allow fair assessment by the Organizing Committee. All contributions will be refereed and the authors will be informed about acceptance and type of presentation by January 31st 1999.

Preparation of Abstracts:
Electronic submission of abstracts is encouraged. These can be generated using our WEB Site at:

http://www.msc.cornell.edu/~ui99

More information on how to submit the abstract can be found on this site.

DEADLINE FOR ABSTRACTS:
30th November 1998.

Further details will be available in due course. All inquiries concerning the Joint Conference shall be addressed to: **Mrs. Suzanne Møller, *UI'99/WCU99* Conference Secretariat, Department of Industrial Acoustics, Technical University of Denmark, Building 425, DK-2800 Lyngby, Denmark, Tel. +45 4525 4766. Fax. +45 4593 0190. E-mail: sm@ipt.dtu.dk**